Environmental adaptation mechanism in marine annelids

Tetsuya Ogino

2019

Contents

General introduction

Marine annelids are segmented worms found in all marine environments from shallow estuaries to rocky shores and to deep-sea sediments, and even swimming in the water column [1]. To date, more than 11,000 species have been described (World Polychaeta Database, http://www.marinespecies.org/polychaeta/) and 25,000 species have been estimated to be exist [2]. Marine annelids are typically existing in great numbers and represented by many species in almost all marine environment [3]. The most of them dwell sediments to make their habitat and to seek their foods. This activity promotes bioturbation and circulation of carbon source and nutrients as well as oxygenation of the sediments. Thus, they play an important role in maintaining marine ecosystems. But, how could marine annelids adapt to various environments?

Environmental adaptation is achieved with the combination of three types of adaptation, morphological, physiological and behavioral adaptation. Morphological adaptation is the process that organisms modify their structure to improve fitness in the environment they inhabit. For example, Tomopteridae, marine annelids swimming in the water column throughout their life, alter their parapodia to achaetous paddle-like shape to improve their ability for swimming [4]. Morphological adaptation is also observed in commensal marine annelids. They modify their appendages to stick on their hosts, i.e. they have hooked setae, sucker-like arching body or host-like appearance [5]. Physiological adaptation is the process of optimization of body chemistry for living in particular environment. The deep-sea hydrothermal vent-endemic worm, alvinellids, are capable of withstanding hot water of more than 50°C [6]. It is an example for physiological adaptation that the temperature of denaturation of alvinellids' collagen fiber is hotter than that of other species [7]. Most of marine annelids confront the threat of seasonal or chronic hypoxia. Marine annelids living in severe hypoxic condition have more enzymes of consuming pyruvate to facilitate anaerobic metabolism [8]. Behavioral adaptation is the process of modification in the behavior that organisms naturally act. The commensal scale worm,

Hesperenoe adventor, lives inside the burrow of fat innkeeper worm, *Urechis caupo*. This scale worm moves back and forth to avoid the peristaltic swelling of the host [9].

As mentioned above, various cases of environmental adaptation of marine annelids have been investigated. However, there is little explanation of their environmental adaptation mechanisms from the molecular biological aspects. In this study, I intend to elucidate the environmental adaptation mechanism of marine annelids focusing on the two species, deep-sea hydrothermal vent-endemic worm, *Paralvinella hessleri* and organically polluted area-endemic worm, *Capitella teleta*. Here, I showed that *P. hessleri* has high chemical sensitivity mediated by transient receptor potential (TRP) channels to minimize the exposure of toxic hydrothermal fluid, and *C. teleta* escapes from their burrow in hypoxia *via* detection of it by TRPA homologue with improving ability to acquire oxygen by changing molecular species of globin genes.

References

1. Daz-Castaeda V, Reish DJ. Polychaetes in environmental studies. In: Shain DH, editor Annelids in modern biology. Wiley-Blackwell; 2009. pp. 203–227.
2. Snelgrove, PVH, Blackburn TH, Hutchings PA, Alongi DM, Grassle JF, Hummel H, et al. The importance of marine sediment biodiversity in ecosystem processes. Ambio. 1997;26: 578–583.
3. Hutchings P. Biodiversity and functioning of polychaetes in benthic sediments. Biodivers Conserv. 1998;7: 1133–1145.
4. Fernández-Álamo MA. Tomopterids (Annelida: Polychaeta) from the eastern tropical Pacific Ocean. Bull Mar Sci. 2000;67: 45–53.
5. Martin D, Britayev TA. Symbiotic polychaetes: review of known species. Ocean Mar Biol Ann Rev. 1998;36: 217–340.
6. Girguis PR, Lee RW. Thermal preference and tolerance of alvinellids. Science. 2006;312: 231.
7. Le Bris N, Gaill F. How does the annelid *Alvinella pompejana* deal with an extreme hydrothermal environment? Rev Environ Sci Biotechnol. 2007;6: 197–221.

8. González RR, Quiñones RA. Pyruvate oxidoreductases involved in glycolytic anaerobic metabolism of polychaetes from the continental shelf off Central-South Chile. Estuar Coast Shelf Sci. 2000;51: 507–519.
9. Dales RP. Interrelations of organisms. A. Commensalism. In: Hedgpeth JW, editors. Treatise on marine ecology and paleoecology. The Geological Society of America Memoir 67; 1957. pp. 391–412.

Chapter 1

High chemical sensitivity of deep-sea hydrothermal vent-endemic annelid, *Paralvinella hessleri.*

Introduction

The environments around deep-sea hydrothermal vents are very harsh for organisms. The vents spout seawater heated by the mantle at temperatures that often reach more than one hundred degrees Centigrade. Moreover, this water is typically acidic, and contains toxic compounds such as heavy metals, hydrogen sulfide and reactive oxygen species [1, 2]. Precipitates of minerals transported by the hydrothermal fluid can form large edifices called chimneys. A large number of invertebrates live on the chimney walls, where they depend on chemosynthetic microbes as a food source or as symbionts [3].

The Annelida worms, Alvinellidae occupy niches near hydrothermal vents. The family Alvinellidae is categorized into two genera, *Alvinella* and *Paralvinella*. They are mainly found in tubes on chimney walls near the blowout ports of vents [4]. Recently, improvements of study methods and tools have made it possible to investigate the physico-chemical conditions of their habitats [5]. These investigations have revealed that the physico-chemical conditions of these habitats are highly fluctuating. *In situ* measurements at an Alvinellidae colony revealed that pH there ranged from 4.4 to 7.5, and temperature from 10ºC to 90ºC [6]. Another survey showed that the temperature inside the tubes on the chimney fluctuated from 28.6ºC to 84.0ºC, while that above the tube openings ranged from 7.5ºC to 40.0ºC [7]. Thus, dealing with the fluctuating physico-chemical conditions in their habitats is key to the survival of Alvinellidae species ("alvinellids"). Several studies have demonstrated behaviors and molecular defenses that contribute to the remarkable thermal tolerance of alvinellids [8-11]. However, little is known about how these worms tolerate the harsh chemical conditions in their environment.

Animals respond to toxic compounds after detecting them with specialized

sensors. Transient receptor potential (TRP) channels are known to be molecular sensors used for such detection by animals ranging from nematodes to mammals [12-14]. TRP channels have been reported to detect various stimuli such as acids, temperature and reactive oxygen species [15-17]. In the environment of hydrothermal vents, many other stimuli exist in addition to these stimuli. For instance, hydrogen sulfide is found there, and is also an activator of TRP channels [18]. These facts suggest that alvinellids may utilize TRP channels for sensing the surrounding chemical environment.

In chapter 1, to reveal the characteristic features of chemical detection in an alvinellid, *Paralvinella hessleri*, the responses of *P. hessleri* to two chemicals, acetic acid and hydrogen peroxide were examined. The low pH of hydrothermal fluid was mainly due to carbonic acid, but hydrochloric acid was also an acid source at some types of hydrothermal vents [19, 20]. I attempted to examine the effect of these acids on the behavior of *P. hessleri*, but it was difficult to prepare acid solutions containing precise concentrations of these acid components because of their volatile nature in addition to the difficulty of handling hydrochloric acid on board research vessels due to its corrosiveness. H^+ sensor involved in acid perception in *P. hessleri* are supposed to respond to various acids, because the sensor would probably recognize H^+ irrespective of the type of acid. Acetic acid was therefore used as a representative acid because acetic acid is often used in nociception tests in crustaceans and mice [21, 22]. Hydrogen peroxide was used as a representative reactive oxygen species (ROS) because it was found at hydrothermal vents. The responses of *P. hessleri* to acetic acid and hydrogen peroxide were compared with those of a related species, *Thelepus* sp., living in the intertidal zone. Finally, I used ruthenium red (RR), a nonselective blocker of TRP channels, to test the involvement of TRP channels in these responses [23, 24]. The findings of this study revealed that *P. hessleri* was highly sensitive to acetic acid and hydrogen peroxide, and TRP channels contributed to the detection of these chemicals.

Materials and methods

Animal collection

Field sampling areas were not protected areas. The study did not involve collecting any endangered or protected species. *Paralvinella hessleri* were collected onboard the research vessel "Natsushima" during research cruise NT12-10 (31°53.05′ N, 139°58.10′ E, 907 m depth, off Myojin-sho submarine caldera, onboard ID 1374–9; or 32°06.21′ N, 139°52.05′ E, 1294 m depth, off Myojin Knoll, onboard ID 1377–4), in the Izu-Ogasawara Arc, Japan. Samples were collected on the 25th or 29th of April 2012 with a remotely operated Hyper-Dolphin 3000 vehicle (HPD#1374 or #1377). A suction sampler was used for collection of *P. hessleri* residing on vent chimneys. The live animals were kept in non-aerated cold deep-sea water collected with the animals. *Thelepus* sp. was collected at the intertidal zone in Osaka prefecture of Japan on the 14th of June 2014. The genus of *Thelepus* sp. was identified according to Fauchald [25].

Chemical avoidance test of *Paralvinella hessleri*

Two glass slides were arranged in parallel with a space of 2-3 millimeters between them. Then another glass slide was put on top of these two slides to cover the space between them, thus creating a tube-like structure imitating the tube that these worms normally inhabit. One individual *P. hessleri* was inserted into "the tube" using its spontaneous backward movement. Ten microliters of inducer (0.01-1% acetic acid, or 0.003-0.3% hydrogen peroxide) were dropped at the opening of the tube (Fig. 1-1). The chemical avoidance behavior was then recorded for 1 min after this induction using a video camera (Panasonic, HX-WA10). Ruthenium red treatment was performed as follows. *Paralvinella hessleri* was submerged in deep-sea water containing 1 mM RR for more than 10 min. Then, the treated worm was moved to a tube for the chemical avoidance test, which was performed as described above.

Chemical avoidance test of *Thelepus* sp.

Thelepus sp. was placed on a plastic Petri dish (AU3100, Eiken Chemical, Tokyo, Japan), and artificial seawater (Rei-sea marine II, Iwaki, Tokyo, Japan) was added to such an extent that the body of the *Thelepus* sp. was partially, but not completely, submerged in seawater. This experimental design was adopted in order to expose the worms directly to inducers. After at least 1 min, recording using a video camera (HX-WA30, Panasonic,

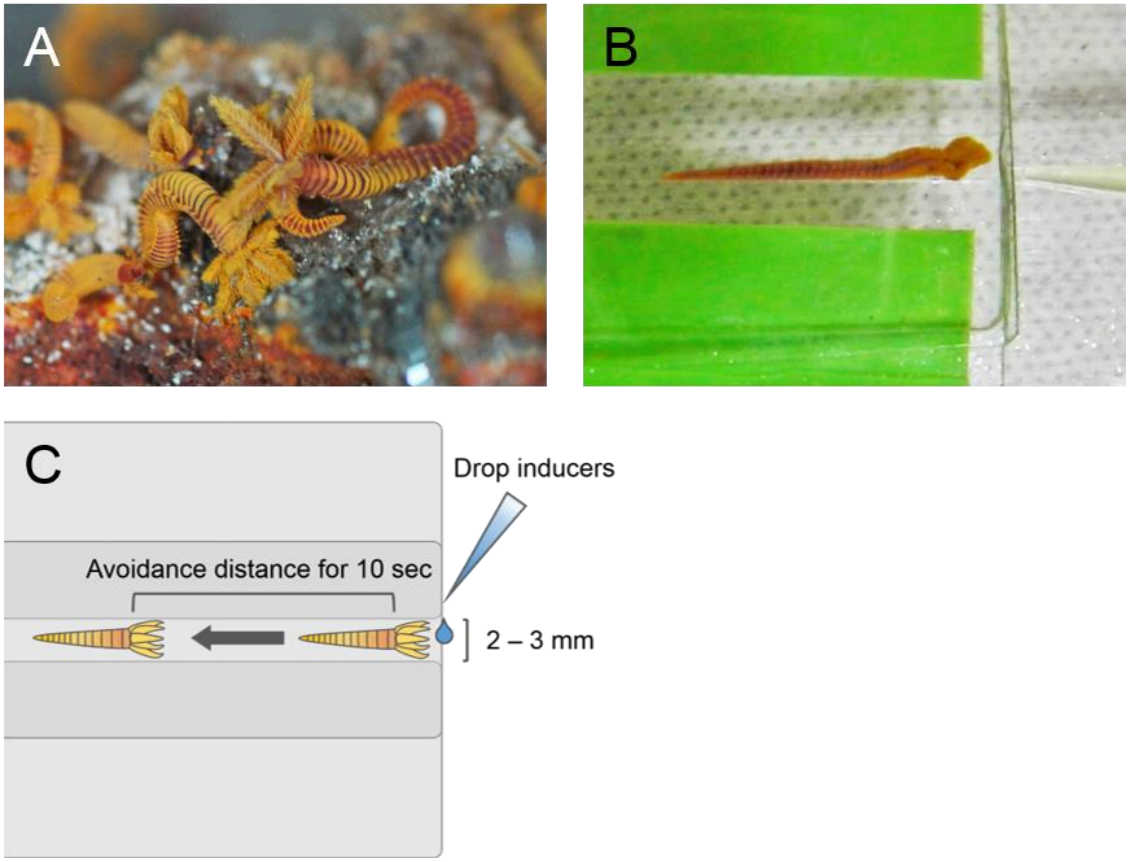

Fig. 1-1. Chemical avoidance test of *Paralvinella hessleri*
(A) Live worms together with the chimney wall they inhabited viewed onboard the research vessel after collection.
(B) A snapshot of the chemical avoidance test of *Paralvinella hessleri.*
(C) A schematic drawing of the chemical avoidance test. A worm was inserted into an artificial tube made of three glass slides imitating a worm's mucous tube. Inducers were dropped at the opening of the tube using a pipette.

Osaka, Japan) was started. The worm's behavior without any treatment was recorded for more than 30 sec, and then 10 μL of inducer (0.01-10% acetic acid or 0.03-30% hydrogen peroxide) was dropped on the worm's head, and its behavior was video-recorded for 1 min. The design of this assay and that performed on *P. hessleri* differed because of the long body size and long tentacles of *Thelepus* sp. For RR treatment, *Thelepus* sp. was submerged in sea water containing 1 mM RR for more than 10 min. Then the treated worm was moved to

a Petri dish and subjected to the chemical avoidance test.

Image analysis

The video images recording the chemical avoidance test of *P. hessleri* were converted from mp4 into AVI format. The coordinates of the head at the start point and 10 sec after induction were determined using DippMotionPro 2D software (DITECT, Tokyo, Japan). The migration distance of each of these head coordinates was calculated as the distance between these two points. The video images of *Thelepus* sp. were also converted from mp4 into AVI format. The coordinates of the head were determined every half-second during the recording using DippMotionPro 2D software. Their migration distances every half-second were calculated using the coordinates' data obtained from the software. The post-induction migration distance minus the pre-induction migration distance was defined as the "avoidance index". The data without RR treatment were analyzed statistically using GraphPad Prism (MDF, Tokyo, Japan) by performing one-way ANOVA followed by Dunnett's multiple comparisons ($p < 0.1$). The statistical significance of the difference between the results obtained with and without RR treatment was determined using Student's *t*-test ($p < 0.1$).

Results

Chemical avoidance test of *Paralvinella hessleri*

To determine the concentrations of acetic acid and hydrogen peroxide that induced chemical avoidance behavior of *P. hessleri*, chemical avoidance tests was conducted. These tests revealed that the avoidance distances of the worm at 0.1% and 1% acetic acid were significantly longer than that for water, while that at 0.01% acetic acid was not (Table 1-1). The avoidance distances of the worm at 0.03% and 0.3% hydrogen peroxide were significantly longer than that for water, while that at 0.003% was not (Table 1-2). Ruthenium red were then used to examine whether TRP channels were involved in the avoidance behavior toward these chemicals. The RR treatment significantly decreased the avoidance distance induced by 0.1% acetic acid and 0.03% hydrogen peroxide ($p < 0.1$) (Tables 1-1 and 1-2).

Table 1-1. Chemical avoidance test of *Paralvinella hessleri* against acetic acid

Concentration (%)	- RR treatment		+ RR treatment	
	Number of samples	Avoidance distance (mm)	Number of samples	Avoidance distance (mm)
0	3	3.19 ± 2.21	ND	ND
0.01	3	0.66 ± 0.66	ND	ND
0.1	3	24.51 ± 12.97*	3	4.93 ± 3.11†
1	3	26.75 ± 6.62*	3	19.81 ± 14.94

Values are mean ± SD; ND: not determined. An asterisk indicates a significant difference between the avoidance distance in the "0" control condition without acetic acid and the avoidance distance with addition of the indicated concentration of acetic acid, as determined by one-way ANOVA with Dunnett's post hoc test ($p < 0.1$). A dagger indicates a significant difference between the avoidance distance with ruthenium red treatment as compared to that without ruthenium red treatment, as determined by Student's *t*-test ($p < 0.1$).

Table 1-2. Chemical avoidance test of *Paralvinella hessleri* against hydrogen peroxide

Concentration (%)	- RR treatment		+ RR treatment	
	Number of samples	Avoidance distance (mm)	Number of samples	Avoidance distance (mm)
0	3	3.19 ± 2.21	ND	ND
0.003	3	1.99 ± 0.40	ND	ND
0.03	3	18.16 ± 8.05*	3	3.84 ± 3.51†
0.3	3	28.07 ± 10.60*	6	22.16 ± 12.07

Values are mean ± SD; ND: not determined. An asterisk indicates a significant difference between the avoidance distance in the "0" control condition without hydrogen peroxide and the avoidance distance with addition of the indicated concentration of hydrogen peroxide, as determined by one-way ANOVA with Dunnett's post hoc test ($p < 0.1$). A dagger indicates a significant difference between the avoidance distance with ruthenium red treatment as compared to that without ruthenium red treatment, as determined by Student's *t*-test ($p < 0.1$).

Chemical avoidance test of *Thelepus* sp.

To compare the sensitivity of *P. hessleri* to chemicals with the sensitivity of related species inhabiting the intertidal zone, chemical avoidance tests on *Thelepus* sp. was conducted. At first, I tried to adopt the method I had used for *P. hessleri*, but this method did not work properly due to the larger body size and longer tentacles of this species. To avoid the difficulty of using the tube-like structure test, I instead measured the movement of the head to evaluate the effects of various chemicals. In this test, I made an effort to drop the chemicals directly on the head in order to apply the same inducing stimulus as that applied in the test for *P. hessleri* as far as possible. The avoidance index of this worm against 10% acetic acid was significantly higher than that against water, while acetic acid at lower concentrations did not affect the avoidance behavior compared to that against water (Table 1-3). The avoidance index of the worm at 30% hydrogen peroxide was significantly higher than that against water, while hydrogen peroxide at lower concentrations did not cause a higher avoidance index compared to water (Table 1-4). To test the possible involvement of TRP channels in the avoidance behavior, the avoidance index of *Thelepus* sp. after RR treatment was examined. RR treatment did not decrease the avoidance index at any concentration of acetic acid tested, but increased the avoidance index at 0.1% acetic acid ($p < 0.1$, Table 1-3). Ruthenium red treatment significantly decreased the avoidance index at 30% hydrogen peroxide ($p < 0.1$, Table 1-4).

Discussion

In chemical avoidance test against acetic acid, *P. hessleri* showed significantly greater avoidance distance at concentrations of 0.1% (pH 3.2) and 1% (pH 2.7) acetic acid (Table 1-1). The hydrothermal fluids released from hydrothermal vents are acidic (around pH 3), while the surrounding water has a stable, slightly alkaline pH (pH 7.8) [26]. These features cause a steep gradient of proton concentration at the boundary between the hydrothermal fluids and surrounding water, namely, at the habitat of *P. hessleri*. Environmental acids cause toxic effects in aquatic animals by disturbing ionic or/and osmotic regulation [27, 28]. Therefore, it seems reasonable to expect that *P. hessleri*

Table 1-3. Chemical avoidance test of *Thelepus* sp. against acetic acid

Concentration (%)	- RR treatment		+ RR treatment	
	Number of samples	Avoidance index (mm)	Number of samples	Avoidance index (mm)
0	5	4.96 ± 5.09	5	3.75 ± 6.16
0.01	5	-0.54 ± 6.13	ND	ND
0.1	5	-1.87 ± 1.36	4	6.21 ± 1.74†
1	5	10.93 ± 10.30	5	18.41 ± 7.02
10	5	28.22 ± 20.94*	5	29.63 ± 16.14

Avoidance index was calculated as the post-induction migration distance during 30 sec minus the pre-induction migration distance during 30 sec. Values are mean ± SD; ND: not determined. An asterisk indicates a significant difference between the avoidance index in the "0" control condition without acetic acid and the avoidance index at the indicated concentration of acetic acid without RR treatment, as determined by one-way ANOVA with Dunnett's post hoc test ($p < 0.1$). A dagger indicates a significant difference between the avoidance index with ruthenium red treatment as compared to that without ruthenium red treatment, as determined by Student's *t*-test ($p < 0.1$).

Table 1-4. Chemical avoidance test of *Thelepus* sp. against hydrogen peroxide

Concentration (%)	- RR treatment		+ RR treatment	
	Number of samples	Avoidance index (mm)	Number of samples	Avoidance index (mm)
0	5	4.96 ± 5.09	5	3.75 ± 6.16
0.03	4	-5.23 ± 6.16	ND	ND
0.3	5	6.98 ± 5.25	5	2.41 ± 2.89
3	7	11.52 ± 9.08	5	19.50 ± 4.57
30	4	32.46 ± 19.20*	4	6.86 ± 13.07†

Avoidance index was calculated as the post-induction migration distance travelled during 30 sec minus the pre-induction migration distance travelled during 30 sec. Values are mean ± SD; ND: not determined. An asterisk indicates a significant difference between the avoidance index in the "0" control condition without hydrogen peroxide and the avoidance index with the indicated concentration of hydrogen peroxide without RR treatment, as determined by one-way ANOVA with Dunnett's post hoc test ($p < 0.1$). A dagger indicates a significant difference between the avoidance index with ruthenium red treatment as compared to that without ruthenium red treatment, as determined by Student's *t*-test ($p < 0.1$).

might monitor environmental protons in order to detect the approach of hazardous hydrothermal fluids. In contrast, the pH of the water which *Thelepus* sp. inhabits is stable and slightly alkaline. Therefore, it is not necessary for *Thelepus* sp. to respond to environmental pH. This is in agreement with the finding that *Thelepus* sp. did not display avoidance behavior over the physiological pH range (Table 1-3).

In the chemical avoidance test against hydrogen peroxide, *P. hessleri* showed significantly increased avoidance distances at 0.03% and 0.3% hydrogen peroxide (Table 1-2). Hydrothermal fluid itself contains no oxygen or ROS such as hydrogen peroxide [26]. However, ROS can be produced when both sulfide and molecular oxygen are present in the surrounding water, suggesting that ROS might be produced at the boundary between hydrothermal fluids and surrounding water [29]. In fact, hydrogen peroxide has been reported to exist in the environment of hydrothermal vents [2]. Because ROS, including hydrogen peroxide, can damage biomolecules [30], it is advantageous for organisms such as *P. hessleri* to be able to sense hydrogen peroxide in order to avoid exposure to it. In the intertidal zone, hydrogen peroxide is produced photochemically, and ranges in concentration from low nM levels to 440 nM in surface seawater [31]. *Thelepus* sp. showed avoidance behavior only toward 30% hydrogen peroxide (Table 1-4). Hydrogen peroxide is not known to be present at such a high concentration in the natural environment of *Thelepus* sp., and hence it is not necessary for *Thelepus* sp. to respond behaviorally to environmental ROS.

Behavioral responses of aquatic animals to environmental acids have been reported so far for fishes [32, 33], crustaceans [34, 35] and mollusks [36, 37]. The contribution of TRP channels to behavioral responses toward low pH was shown in nematode [15], suggesting the possible involvement of TRP channels in the behavioral response to acids in other aquatic animals as well. In contrast, behavioral responses of aquatic animals toward environmental ROS have never been reported. However, TRP channels were shown to be involved in the detection of hydrogen peroxide in mouse [38], suggesting the possibility that TRP channels might be involved in the behavioral response to hydrogen peroxide in aquatic animals. In the chemical avoidance test in the present study, *P. hessleri* and *Thelepus* sp. responded to acids

and hydrogen peroxide. To test the involvement of TRP channels in the behavioral response to acids and hydrogen peroxide, chemical avoidance tests were conducted after the administration of a non-selective TRP channel blocker, ruthenium red.

Ruthenium red treatment significantly decreased the avoidance distance of *P. hessleri* against 0.1% acetic acid and 0.03% hydrogen peroxide but not against higher concentrations (Tables 1-1 and 1-2), indicating that TRP channels mediated the detection by *P. hessleri* of toxic chemicals at low, but not high, concentrations. These results imply that receptors other rather than TRP channels are involved in the detection of acetic acid and hydrogen peroxide at such higher concentrations. TRP channels and ryanodine receptors (RyRs) are Ca^{2+} channel proteins that may be involved in animal behavior, and RR is known to be an antagonist against these Ca^{2+} channels [39, 40]. RyRs function to release Ca^{2+} from the sarcoplasmic reticulum and to induce muscle contraction [41], suggesting that muscle contraction would be suppressed in an animal if RR inhibited the animal's Ca^{2+} transport through RyRs. In the present study, however, RR showed no inhibitory effect on the body movement associated with muscle contraction on either species examined, which suggests that RR does not have an antagonistic effect against RyRs of either species. This might be because the rate of permeation of RR into the animals was so slow [40] that RR did not reach RyRs in muscle and only reacted with Ca^{2+} channels localized in the skin during the experimental period.

The TRP channel family consists of many members and is divided into several subfamilies [23]. In mammals, TRPV1, TRPA1 and some other members of the TRP channel family have been reported to be activated by protons [42, 43]. *Caenorhabditis elegans* shows avoidance behavior against acidic pH (pH 3-5), which is detected in this animal by OSM-9, a member of the TRPV subfamily [15]. Interestingly, this pH is close to that which induces avoidance behavior of *P. hessleri*, which implies that similar TRP channels may be involved in the acid avoidance of *P. hessleri*. Reactive oxygen species, including hydrogen peroxide, are detected by mammals *via* TRPA1 [17, 38], TRPM2 [44] and some other members of the TRP family [45]. I speculate that homologue of these TRP channels are possible candidates for the hydrogen peroxide sensor of *P. hessleri*. Further

studies will be needed to identify the particular TRP channels that act as chemical sensors in *P. hessleri* and to clarify their functions.

This newly developed assay reported here can easily evaluate the avoidance behavior of a deep-sea hydrothermal vent animal, *P. hessleri*, onboard a research vessel. The findings here using this assay revealed that *P. hessleri* showed avoidance behavior against two environmentally relevant inducers with high sensitivity. Its ability to escape from toxic chemicals even at low concentrations should contribute to its ability to occupy a niche in the vicinity of hydrothermal vents. In addition, our results suggested that TRP channels act as sensors of these chemicals. Further studies are needed to identify the particular TRP channels that act as chemical sensors and clarify their functions in hydrothermal vent animals, which will lead to unraveling the chemical sensing mechanisms of these animals.

References

1. Von Damn KL. Seafloor hydrothermal activity: black smoker chemistry and chimneys. Annu Rev Earth Planet Sci. 1990;18: 173-204.
2. Luther GW, Rozan TF, Taillefert M, Nuzzio DB, Di Meo C, Shank TM, et al. Chemical speciation drives hydrothermal vent ecology. Nature. 2001;410: 813-816.
3. Lutz RA, Kennish MJ. Ecology of deep-sea hydrothermal vent communities: A review. Rev Geophys. 1993;31: 211-242.
4. Desbruyères D, Segonzac M, Bright M. Handbook of deep-sea hydrothermal vent fauna. 2nd ed. Linz Denisia; 2006. p. 287.
5. Le Bris N, Gaill F. How does the annelid *Alvnella pompejana* deal with an extreme hydrothermal environment? Rev Environ Sci Biotechnol. 2007;6: 197-221.
6. Le Bris N, Sarradin PM, Pennec S. A new deep-sea probe for in situ pH measurement in the environment of hydrothermal vent biological communities. Deep Sea Res Part I. 2001;48: 1941-1951.
7. Di Meo-Savoie CA, Luther GW, Cary SC. Physicochemical characterization of the microhabitat of the epibionts associated with *Alvinella pompejana*, a hydrothermal vent

annelid. Geochim Cosmochim Acta. 2004;68: 2055-2066.

8. Girguis PR, Lee RW. Thermal preference and tolerance of alvinellids. Science. 2006;312: 231.
9. Dilly GF, Young R, Lane WS, Pangilinan J, Girguis PR. Exploring the limit of metazoan thermal tolerance via comparative proteomics: thermally induced changes in protein abundance by two hydrothermal vent polychaetes. Proc R Soc B. 2012;279: 3347-3356.
10. Cary SC, Shank T, Stein JR. Worms bask in extreme temperatures. Nat Chem. 1998;391: 545-546.
11. Gaill F, Mann K, Wiedemann H, Engel J, Timpl R. Structural comparison of cuticle and interstitial collagens from annelids living in shallow sea-water and at deep-sea hydrothermal vents. J Mol Biol. 1995;246: 284-294.
12. Harteneck C, Plant TD, Schultz G. From worm to man: three subfamilies of TRP channels. Trends Neurosci. 2000;23: 159-166.
13. Montell C. Drosophila TRP channels. Eur J Physiol. 2005;451: 19-28.
14. Clapham DE. TRP channels as cellular sensors. Nature. 2003;426: 517-524.
15. Sambongi Y, Takeda K, Wakabayashi T, Ueda I, Wada Y, Futai M. *Caenorhabditis elegans* senses protons through amphid chemosensory neurons: proton signals elicit avoidance behavior. Neuroreport. 2000;11: 2229-2232.
16. Caterina MJ, Schumacher MA, Tominaga M, Rosen TA, Levine JD, Julius D. The capsaicin receptor: a heat-activated ion channel in the pain pathway. Nature, 1997;389: 816-24.
17. Andersson DA, Gentry C, Moss S, Bevan S. Transient receptor potential A1 is a sensory receptor for multiple products of oxidative stress. J Neurosci. 2008;28: 2485-2494.
18. Trevisani M, Patacchini R, Nicoletti P, Gatti R, Gazzieri D, Lissi N, et al. Hydrogen sulfide causes vanilloid receptor 1-mediated neurogenic inflammation in the airways. Br J Pharmacol. 2005;145: 1123-1131.
19. Tsunogai U, Ishibashi J, Wakita H, Gamo T, Watanabe K, Kajimura T, et al. Peculiar

features of Suiyo Seamount hydrothermal fluids, Izu-Bonin Arc: Differences from subaerial volcanism. Earth Planet Sci Lett. 1994;126: 289-301.

20. Edmond JM, Measures C, McDuff RE, Chan LH, Collier R, Grant B, et al. Ridge crest hydrothermal activity and the balances of the major and minor elements in the ocean: The Galapagos data. Earth Planet Sci Lett. 1979;46: 1-18.
21. Barr S, Laming PR, Dick JTA, Elwood RW. Nociception or pain in a decapod crustacean? Anim Behav. 2008;75: 745-751.
22. Ribeiro RA, Vale ML, Thomazzi SM, Paschoalato ABP, Poole S, Ferreira SH, et al. Involvement of resident macrophages and mast cells in the writhing nociceptive response induced by zymosan and acetic acid in mice. Eur J Pharmacol. 2000;387: 111-118.
23. Clapham DE, Runnels LW, Strübing C. The TRP ion channel family. Nat Rev Neurosci. 2001;2: 387-396.
24. Amann R, Maggi CA. Ruthenium red as a capsaicin antagonist. Life Sci. 1991;49: 849-856.
25. Fauchald K. The Polychaete worms, definitions and keys to the orders, families and genera. Natural History Museum of Los Angeles Country; 1977. pp. 118-134.
26. Hourdez S, Lallier FH. Adaptations to hypoxia in hydrothermal vent and cold-seep invertebrates. Rev Environ Sci Biotehnol. 2007;6: 143-159.
27. Lignot JH, Spanings-Pierrot C, Charmantier G. Osmoregulatory capacity as a tool in monitoring the physiological condition and the effect of stress in crustaceans. Aquaculture. 2000;191: 209-245.
28. Pynnönen K. Influence of aluminum and H^+ on the electrolyte homeostasis in the Unionidae *Anodonta anatina* L. and *Unio pictorum* L. Arch Environ Contam Toxicol. 1991;20: 218-225.
29. Tapley DW, Buettner GR, Shick JM. Free radicals and chemiluminescence as products of the spontaneous oxidation of sulfide in seawater, and their biological implication. Biol Bull. 1999;196: 52-56.
30. Lesser MP. Oxidative stress in marine environments: biochemistry and physiological

ecology. Annu Rev Physiol. 2006;68: 253-78.

31. Clark CD, De Bruyn WJ, Jakubowski SD, Grant SB. Hydrogen peroxide production in marine bathing waters: Implications for fecal indicator bacteria mortality. Mar Pollut Bull. 2008;56: 397-401.
32. Ikuta K, Suzuki Y, Kitamura S. Effects of low pH on the reproductive behavior of salmonid fishes. Fish Physiol Biochem. 2003;28: 407-410.
33. Kroon F. Behavioural avoidance of acidified water by juveniles of four commercial fish and prawn species with migratory life stages. Mar Ecol Prog Ser. 2005;285: 193-204.
34. De la Haye KL, Spicer JI, Widdicombe S, Briffa M. Reduced pH sea water disrupts chemo-responsive behaviour in an intertidal crustacean. J Exp Mar Bio Ecol. 2012;412: 134-140.
35. Felten V, Charmantier G, Charmantier-Daures M, Aujoulat F, Garric J, Geffard O. Physiological and behavioural responses of *Gammarus pulex* exposed to acid stress. Comp Biochem Physiol Part C Toxicol Pharmacol. 2008;147: 189-197.
36. Bamber RN. The effects of acidic seawater on three species of lamellibranch mollusc. J Exp Mar Bio Ecol. 1990;143: 181-191.
37. Dove MC, Sammut J. Histological and feeding response of Sydney rock oysters, *Saccostrea glomerata*, to acid sulfate soil outflows. J Shellfish Res. 2007;26: 509-518.
38. Sawada Y, Hosokawa H, Matsumura K, Kobayashi S. Activation of transient receptor potential ankyrin 1 by hydrogen peroxide. Eur J Neurosci. 2008;27: 1131-1142.
39. Saito S, Hamanaka G, Kawai N, Furukawa R, Gojobori J. Characterization of TRPA channels in the starfish *Patiria pectinifera*: involvement of thermally activated TRPA1 in thermotaxis in marine planktonic larvae. Sci Rep. 2017;1-14.
40. Baylor, SM, Hollingworth S, Marshall MW. Effects of intracellular ruthenium red on excitation-contraction coupling in intact frog skeletal muscle fibres. J Physiol. 1989;408: 617-635.
41. Fill M, Copello JA. Ryanodine receptor calcium release channels. Physiol Rev. 2002;82: 893-922.

42. Jordt SE, Tominaga M, Julius D. Acid potentiation of the capsaicin receptor determined by a key extracellular site. Proc Natl Acad Sci. 2000;97: 8134-8139.
43. Takahashi N, Mizuno Y, Kozai D, Yamamoto S, Kiyonaka S, Shibata T, et al. Molecular characterization of TRPA1 channel activation by cysteine-reactive inflammatory mediators. Channels. 2008;2: 1-12.
44. Kaneko S, Kawakami S, Hara Y, Wakamori M, Itoh E, Minami T, et al. A critical role of TRPM2 in neuronal cell death by hydrogen peroxide. J Pharmacol Sci. 2006;101: 66–76.
45. Hara Y, Wakamori M, Ishii M, Maeno E, Nishida M, Yoshida T, et al. LTRPC2 Ca2+-Permeable channel activated by changes in redox status confers susceptibility to cell death. Mol Cell. 2002;9: 163-173.

Chapter 2

Exploration of the hypoxia sensor for behavioral response in marine annelid, *Capitella teleta*.

Introduction

Hypoxic zones are expanding in open oceans and coastal waters due to global warming and high nutrient inputs, and have influences on ecosystems and biodiversity [1-3]. This expansion is considered likely to continue, and to have unpredictable impacts on marine animals, including species commercially important for fishing. Hypoxia is conventionally defined as dissolved oxygen concentration (DO) < 2 mg/L. The effects of hypoxia vary depending on the species, although they are roughly similar within a particular taxonomic group, and reflect differences in animals' behavioral and physiological adaptability to hypoxia [4, 5]. It is important to clearly understand the influence of hypoxia on marine benthic animals, because these animals have important roles in supporting marine ecology.

Marine annelids of the genus *Capitella* are small, thread-like worms with hypoxia tolerance [6]. They inhabit organically polluted sediment in coastal water, where severe hypoxia occurs in summer [7, 8]. Their population shows rapid growth prior to other species in autumn as DO rises [8, 9]. Therefore, they are thought to respond sensitively to the fluctuation of DO and to return to the habitat rapidly as DO rises.

Responses of marine invertebrates to hypoxia can be simply categorized into physiological and behavioral responses [1, 10]. The physiological responses are promotion of hemoglobin synthesis [11] and enhancement of the anaerobic metabolism [12-14]. Hypoxia inducible factors (HIFs) play regulatory functions in these responses, and their mechanism of regulation is well understood in terrestrial organisms [15-17]. The regulation of physiological responses by HIFs are also observed in marine animals such as bivalves, crustaceans and fish [18-21]. On the other hand, the behavioral responses include avoidance

of hypoxic water [22, 23] and suppression of heartbeat rates [24]. However, there is little knowledge about the hypoxia sensing system that regulates behavioral responses in marine invertebrates.

Recently, in mammals, one member of the transient receptor potential channel family, TRPA1, was reported to be involved in the hypoxia detection system and to regulate hypoxia-triggered behavioral responses [25, 26]. In this chapter, I showed that TRPA homologue possibly contributes to the hypoxia-detection system of marine invertebrates, as indicated by the experiments on hypoxia-avoidance behavior of *C. teleta*.

Materials and methods

Rearing of *Capitella teleta*

Stock cultures of *C. teleta* were kindly provided by Dr. H. Tsutsumi of Prefectural University of Kumamoto and Dr. N. Ueda of the University of Kitakyushu, and reared in mud with artificial sea water (ASW) (Rei-sea marine II, Iwaki, Tokyo, Japan) of 33 psu salinity at 18°C. The worms were originally collected from the sediment below a fish farm (32°23’52 N, 130°13’40 E) or Dokai Bay (33°52’34 N, 130°45’3 E). Worms were fed commercial fish food.

Hypoxia avoidance assay

Ten mL of glass beads (BZ-01, AS ONE Corporation, Osaka, Japan) and 50 mL of ASW were poured into glass vials (No.7L, AS ONE Corporation). Ten bare worms were transferred into the vials and kept for more than 3 h at room temperature. Stock solutions of 100 mM A-967079 (Wako Pure Chemical Industries, Ltd., Osaka, Japan) were made in DMSO and stored at -30°C until use. Five μL of A-967079 stock solution was added to the ASW in each glass vial containing worms, making a final concentration of 10 μM, while in control treatments, DMSO alone was added. To ensure the inhibitory effect of A-967079, these vials were kept for 10 min. Hypoxia was achieved by blowing nitrogen gas into the solution for 10 min. Then the cap was closed and vials were allowed to stand for 8 h, during which photographs were taken every 30 min. Hypoxia-avoidance behavior was evaluated by the number of worms of which part protruded from the glass beads. This experiment was

repeated 10 times. Real-time monitoring of DO could not be done to avoid disturbing the environmental condition in the vial. Therefore, the same experiments as above without A-967079 treatment were conducted only to measure DO. Dissolved oxygen concentrations at 0 h, 4 h and 8 h were measured using a Seven2Go DO meter (METTLER TOLEDO, Columbus, USA). The measurements were repeated three times.

Effect of A-967079 on worm locomotor activity

The bare worms were rinsed with ASW and transferred to a dish with diameter 8.75 cm containing 25 mL ASW supplemented with 0.01% 100 mM A-967079 dissolved in DMSO (final 10 μM A-967069) or 0.01% DMSO as mock control. Photographs were taken with a WG-5 GPS camera (RICOH, Tokyo, Japan) at the rate of one photograph/min for 42 min immediately after transfer. The coordinates of the head of worms were estimated using ImageJ [27]. Their migration distance during 30 min was calculated to determine the effect of A-967079 on their locomotor activity. This analysis was done using the 11th to 41st photograph because the first 10 min was taken as the time to ensure the inhibitory effect of A-9670679. The number of replications of A-967079 treatment was 12, while that of the mock control was 13.

Cloning, domain structure and phylogenetic analysis of CtTRPAbasal

A part of the TRPA gene sequence from *C. teleta* was acquired by BLAST search using the human TRPA1 protein sequence (NP_0015628.2) as query. The Sequence ID of the most similar protein sequence is ELT91340.1. The sequence of full-length CtTRPAbasal was determined by the rapid amplification of cDNA ends method, and the open reading frame with flanking regions was cloned with two primers containing restriction enzyme sites at the 5'ends; Fw: ACTAAAGCTTTAACGCTGCATCAGTGCG CTCG, Rv; ACTAGGATCCTAACCAGACAACGGCTTGAAAC. This was amplified using KOD Plus Neo (TOYOBO, Osaka, Japan) with the following program; initial incubation at 94°C for 2 min; 35 cycles of denaturation at 98°C for 10 sec, annealing at 60°C for 30 sec and amplification at 68°C for 3.5 min, and final incubation at 68°C for 5 min. Amplified products were cut with *Bam*HI and *Hind*III and inserted into pBluescript KS(-).

The domain structure of CtTRPAbasal was analyzed using InterProScan [28]. Phylogenic analysis was performed using MEGA7 [29]. Gene IDs used for phylogenic analysis of CtTRPAbasal are listed in Table 2-1. Transmembrane regions in the deduced amino acid sequence of these genes were determined using Pfam search [30] and aligned by using MUSCLE [31]. A phylogenic tree was constructed by the maximum likelihood method using the LG model. A discrete gamma distribution was used to model evolutionary rate differences among sites (5 categories (+*G*, parameter = 1.3532)). The gaps were completely deleted. The oxygen-dependent degradation domain (ODD) of CtTRPAbasal was deduced by alignment with the ODD from human HIF-1α and HIF-2α [32] using ClustalW [33]. Analysis of the alignment was performed using Jalview [34].

Table 2-1. Gene accession number used for phylogenic analysis

Sequence name in the tree	Accession number
Caenorhabditis elegans	NP_502249.3
Drosophila melanogaster painless	NP_611979
Drosophila melanogaster pyrexia	NP_612015
Drosophila melanogaster water witch	NP_731193
Drosophila melanogaster TRPA1	NP_648263
Danio rerio	XP_009296845
Gallus gallus	BAO51998
Homo sapiens	NP_015628
Mus musculus	NP_808449
Python regius	ADD82928
Xenopus tropicalis	NP_001121434
Anopheles gambiae	ACC86138
Patiria pectinifera TRPA basal	BAX76613.1
Patiria pectinifera TRPA1	BAX76612.1

Whole-mount *in situ* hybridization

Worms were kept in a 0.5% agar plate buffered with ASW for 2 days to remove the mud inside the gut. Then, the worms were relaxed in 1:1 0.37 M $MgCl_2$:ASW for more than 10 min. Relaxed worms were fixed with 4% paraformaldehyde (PFA)/PBS overnight at 4°C. Dehydration was achieved as follows: incubation in 25% methanol/75% PBS for 5 min, 50% methanol/50% PBS for 5 min, 75% methanol/25% PBS for 5 min, 100% methanol twice for 10 min each, and the dehydrated samples were then stored at -20°C until experiments.

Samples were rehydrated with 75% methanol/25% PBST (PBS, 0.1 % Tween 20) for 5 min, 50% methanol/50% PBST for 5 min, 25% methanol/75% PBST for 5 min and 3 times with PBST for 5 min each, and then digested with protease K (10 μg/mL) in PBST for 30 min at room temperature. After washing with PBST, samples were soaked in 0.1 M triethanolamine (pH 7-8) for 5 min to inactivate endogenous alkaline phosphatase. Then the samples were transferred to fresh 0.1 M triethanolamine and 1/400 volume of acetic anhydride was added to block the nonspecific binding of probes. Five minutes later, another 1/400 volume of acetic anhydride was added and the samples were incubated for 5 min. Then, samples were washed two times with PBST for 5 min and fixed with 4% PFA for 1 h followed by three washes with PBST for 5 min. Samples were washed with hybridization buffer (Hyb; 50% formamide, 5×SSC, 50 μg/mL heparin, 0.1% Tween 20, 1% SDS, 100 μg/mL ribonucleic acid from torula yeast), and then prehybridized with fresh hybridization buffer for 2 h at 65°C. Digoxigenin-labeled RNA probes were synthesized using a DIG RNA Labeling Kit (Roche, Basel, Switzerland) (with T3 for antisense probe and T7 for sense probe). The template was 521 bp from 1945 to 2466 bp in the open reading frame of CtTRPAbasal cloned into pBluescript KS (-). Hybridization was carried out using probes at 0.1 ng/μL overnight at 65°C. After hybridization, worms were washed with Hyb for 5 min and then for 20 min, 2 times with 75% Hyb/25% PBST for 20 min, 2 times with 50% Hyb/50% PBST for 20 min and 2 times with 25% Hyb/75% PBST for 20 min at 65°C, and then 3 times with PBST for 5 min and 5 times with PBT (1 × PBS, 0.2% TritonX-100, 0.1% BSA). Riboprobes were visualized as follows: samples were incubated for 1 h with

blocking buffer (10 × blocking buffer (Roche) diluted to 1 × conc. by PBS), then overnight with anti-Digoxygenin Fab Fragment (Roche) diluted 1:5000 in blocking buffer at 4°C, and then washed 3 times with PBT for 5 min. Color development was carried out using BM-Purple (Roche). Colored samples were then equilibrated in 80% glycerol/PBS and images were captured with VB-7000 (KEYENCE, Osaka, Japan) mounted on MZFLIII (Leica Microsystems, Wetzlar, Germany). Image stacking of multiple focal planes was performed with ImageJ.

Results

Hypoxia avoidance assay

To examine the involvement of TRPA1 in hypoxia detection by *C. teleta*, the effects of a TRPA1-specific inhibitor, A-967079, on the hypoxia-induced response were examined (Fig. 2-1). The worms exposed to severe hypoxic conditions crawled out of the sediment, and the number of worms showing this behavior in severe hypoxia treatment was significantly larger than that in normoxia treatment at every time point examined except for 2.0 and 3.0 h. This behavior was suppressed by 10 μM A-967079 at 0.5, 1.0, 1.5, 6.0, and 7.5 h.

To determine the concentration of DO in the hypoxia avoidance assay, the same experiment as above without A-967079 treatment was conducted three times for measuring DO concentrations. The concentrations of DO in the normoxia treatment were 5.80, 5.91, 5.95 mg/L at 0 h, 2.95, 3.46, 3.60 mg/L at 4 h and 3.57, 3.68, 4.26, mg/L at 8h. In the hypoxia treatment, the concentrations of DO were 0.39, 0.41, 0.46 mg/L at 0 h, 1.24, 1.66, 1.82 mg/L at 4 h and 1.71, 1.80, 1.87 mg/L at 8 h. Throughout this experiment, the temperature was in the range of 24.0 - 24.9°C.

Effect of A-967079 on the locomotor activity

To ensure that A-967079 has no side effect on the worms' locomotor activity, the migration distances (measured at the tip of their head) with or without A-967079 were evaluated (Fig. 2-2). The average migration distance (mm) ± S.D. with A-967079 treatment

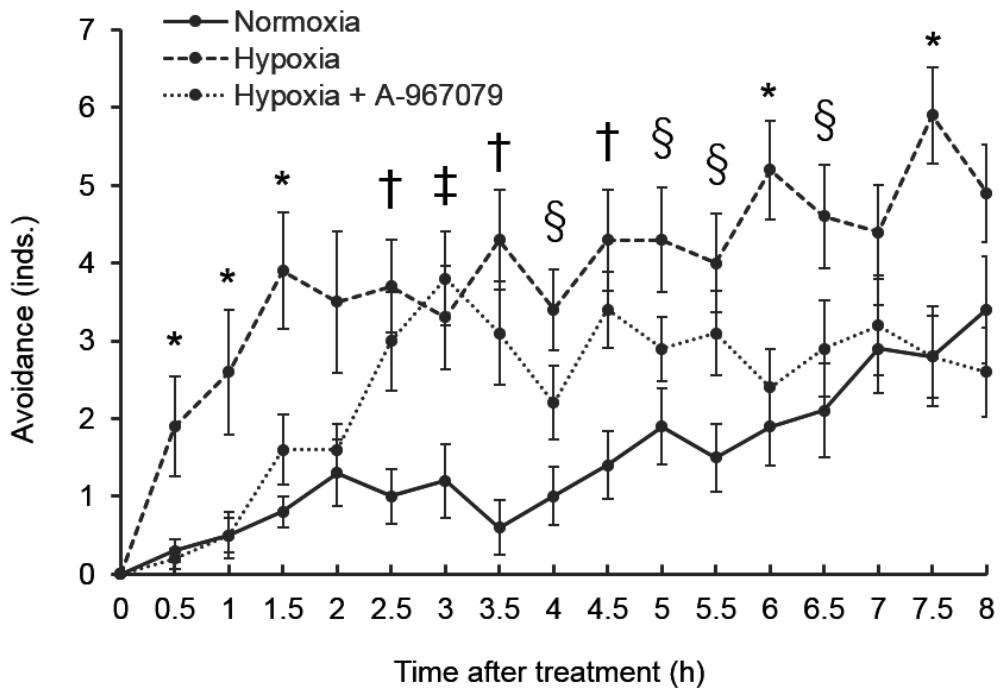

Fig. 2-1. Hypoxia avoidance assay
Values are shown as mean ± SEM of the number of worms that protruded from the glass beads (n = 10). Symbols within this figure indicates the statistically significant differences determined by ANOVA followed by Tukey's test ($p < 0.05$) as follows: *, Hypoxia vs Normoxia or Hypoxia + A-967079; †, Normoxia vs Hypoxia or Hypoxia + A-967079; ‡, Normoxia vs Hypoxia + A-967079; §, Hypoxia vs Normoxia.

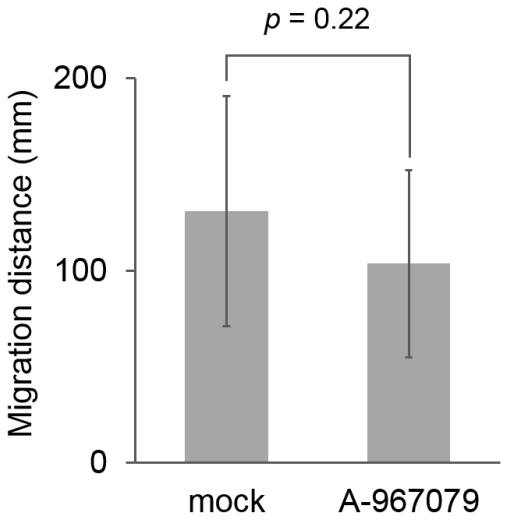

Fig. 2-2. Effect of A-967079 on locomotor activity
Migration distance of the head of *Capitella teleta* for 30 min is shown when they were immersed in artificial seawater with or without 10 μM A-967079. Data are shown as mean ± SD. The data of the two groups were statistically analyzed by Student's *t*-test.

was 103.6 ± 48.7, while that with the mock treatment was 131.0 ± 56.0. The *p*-value between the two treatments evaluated by Student's *t*-test was 0.22.

Domain structure and phylogenic analysis of CtTRPAbasal

To speculate about the function of CtTRPAbasal, its domain structure and phylogeny were examined. The phylogenic relationship of CtTRPAbasal with TRPA from various species from nematode to man was analyzed (Fig. 2-3). This analysis showed that CtTRPAbasal belongs to the same clade as nematode's TRPA [35] and TRPAbasal found in the starfish *Patiria pectinifera* [36]. Many ankyrin repeats in the N-terminal cytosolic region are a typical feature of TRPA, and CtTRPAbasal is speculated to have 16 ankyrin repeats there. The ODD has an important role in the detection of hypoxia in mammalian TRPA1 [25]. To confirm the presence of ODD in CtTRPAbasal, amino acid sequences of ODDs in human HIF-1α and HIF-2α were aligned with CtTRPAbasal, and ODD was found in the N-terminal cytosolic region of CtTRPAbasal (Fig. 2-4).

Whole-mount *in situ* hybridization

To identify where in the worm CtTRPAbasal works, *in situ* hybridization analysis were performed. A strong, sharply defined signal was observed at the prostomium, and a vague signal was observed in the posterior region (Fig. 2-5). However, a sense probe used as a negative control also produced a signal in the posterior region. Therefore, the true signal was concluded to be at the prostomium. The signal in the prostomium was located on both sides as seen from the ventral view.

Discussion

Hypoxia treatment induced escape behavior of *C. teleta*, and this behavior was suppressed by the administration of A-967079 (Fig. 2-1), while the locomotor activity was not suppressed by A-967079 (Fig. 2-2). The suppression of escape behavior in *C. teleta* was prominent at the beginning of the experiment, which suggests that A-967079 influenced a rapid response to hypoxia. In mice, TRPA1 is the key regulator of the hypoxia ventilatory response, i.e., of the increase in ventilation during hypoxia [26]. When mice breathe

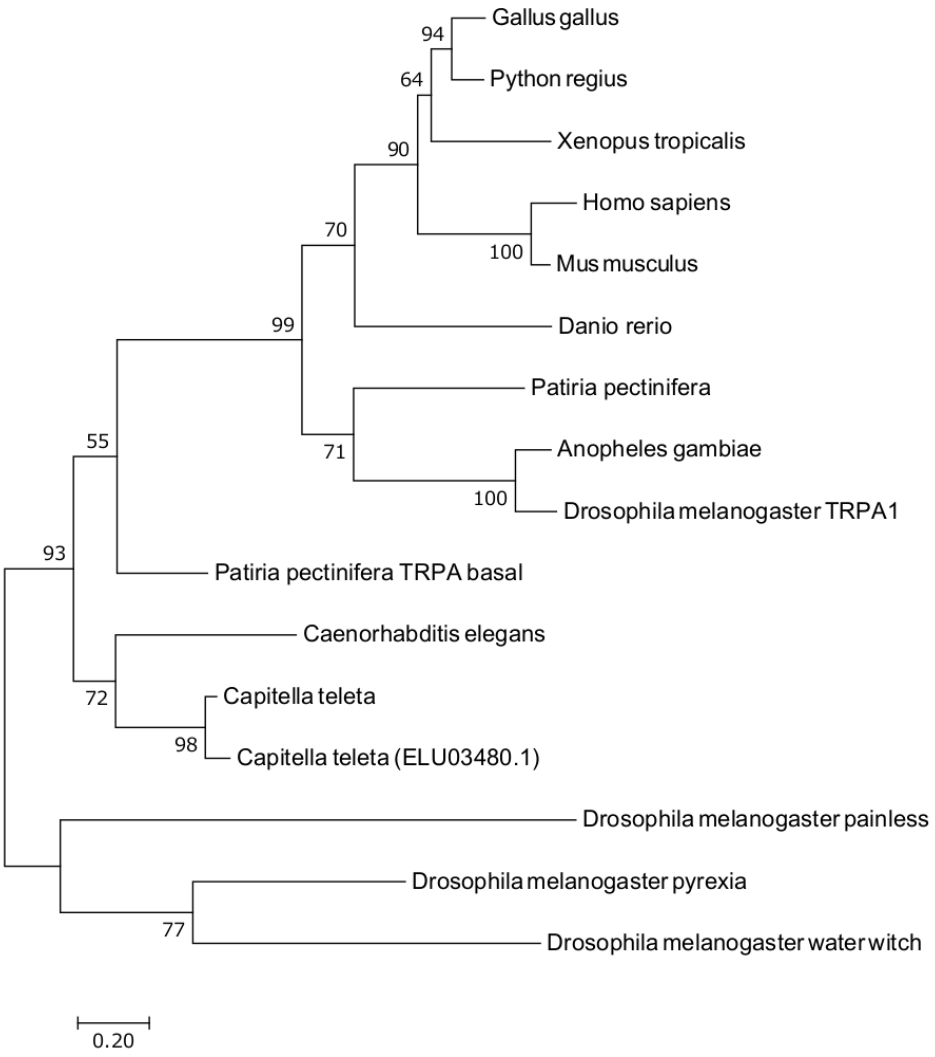

Fig. 2-3. Phylogenic position of CtTRPAbasal

Phylogenic tree of known TRPA channels was constructed by the Maximum likelihood method. Only transmembrane domains were used for constructing the tree. Bootstrap values calculated using 1000 replications are shown near the nodes. Gene accession numbers of the amino acid sequences used in this analysis are shown in Table 2-1.

Fig. 2-4. Alignment of oxygen-dependent degradation domain of human HIFα with that of CtTRPAbasal
The amino acid sequences of HIF-1α and 2α were acquired from NCBI, and the gene accession numbers were Q16665.1 and Q99814.3, respectively. Alignment was done using ClustalW services and the result was analyzed using Jalview. Coloring of amino acids was performed according to ClustalX. Arrowhead indicates the hydroxylation site.

hypoxic air, their respiratory rate increases rapidly, but that of TRPA1-inhibited mice does not. This is in accord with our results, which implied that TRPA1 was involved in the rapid behavioral response to hypoxia. At later time points, A-967079 also suppressed the hypoxia-escaping behavior. Hatano et al. (2012) showed that human TRPA1 was upregulated within several hours by activated HIF-1α, a hypoxia-responsive transcription factor [37]. This suggests that the input of sensing hypoxia *via* the TRPA1 homologue could gradually increase as the time of exposure to hypoxia increased. This might explain our observation that the suppression of the escape behavior reemerged in the late part of this experiment. In the middle part of this experiment, this suppression was not observed. This might be because other hypoxia-sensing mechanisms, such as soluble guanylyl cyclase (sGC) or HIF pathways, overwhelmed the A-967079-induced TRPA1 inhibition.

Similar hypoxia-induced evacuation from sediment is observed in infaunal benthic species. The burrowing marine annelids *Hediste diversicolor* and *Alitta virens* expose themselves on the sediment in response to hypoxia [38]. *Lomia medusa*, a tubicolous

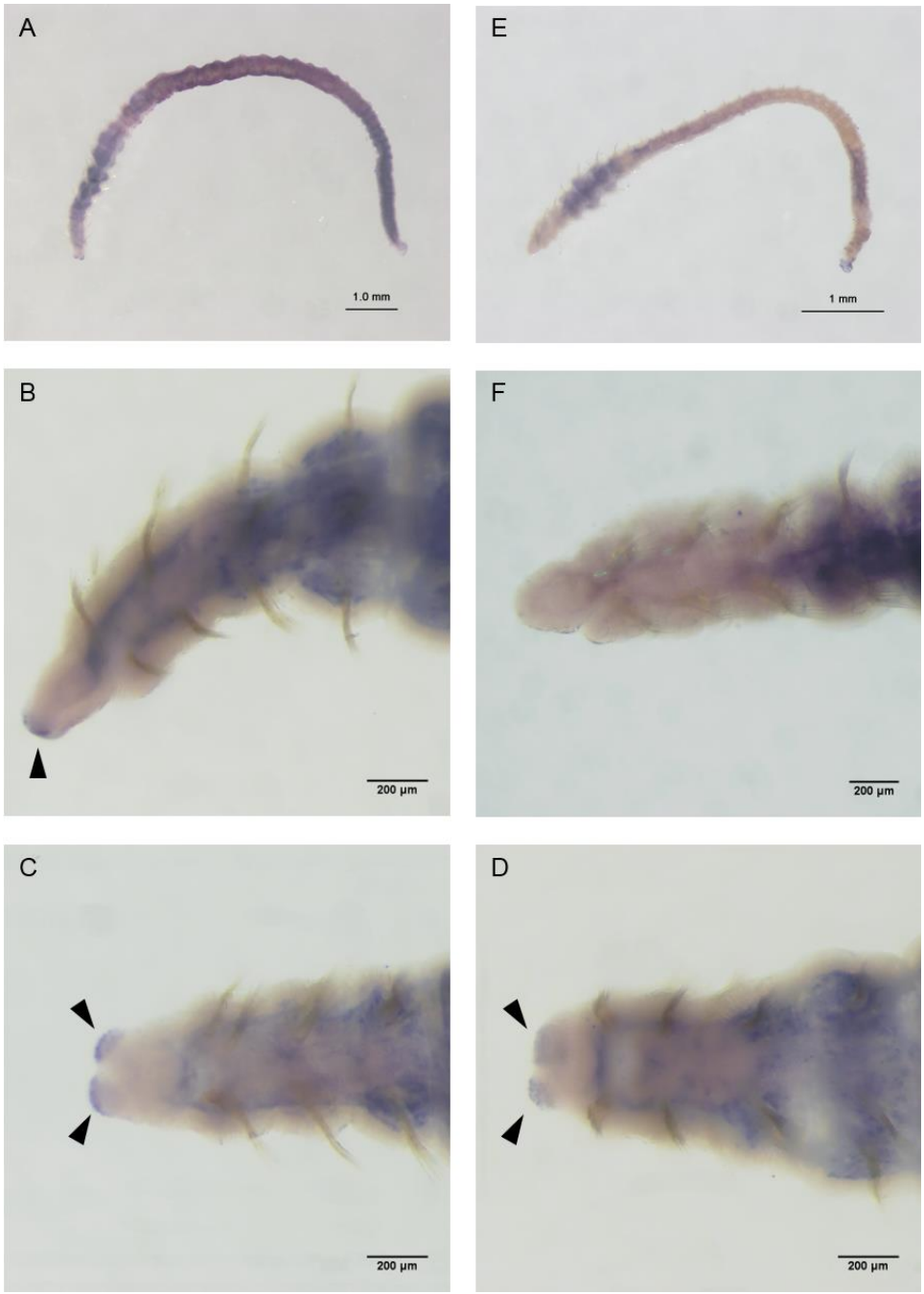

Fig. 2-5. Whole-mount *in situ* hybridization
The probe consisted of 521bp from bp 1945 to bp 2466 in the open reading frame of CtTRPA. Signals were developed using BM-Purple (blue color). Arrowheads indicate the signals at the prostomium. **(A)** Whole body from lateral side with anti-sense probe. **(B)** Lateral side of the head with anti-sense probe. **(C)** Ventral side of the head with anti-sense probe **(D)** Dorsal side of the head with anti-sense probe. **(E)** Whole body from lateral side with sense probe. **(F)** Lateral side of the head with sense probe.

marine annelid, escapes from its tubes in hypoxic conditions [39]. The brittle stars *Amphiura filiformis* and *A. chiajei*, the deposit-feeding bivalves *Abra alba* and *A. nitida*, and the suspension-feeding bivalve *Cerastoderma edule* come out from sediment in response to hypoxic stimuli [40]. In this study, *C. teleta* climbed on the sides of glass vials with their mucous in response to hypoxia. I infer that when they are confronted by hypoxia in their natural habitat, they would crawl out of their burrow and migrate on the surface of sediment to find a more suitable condition. Terrestrial model organisms also show similar hypoxia-induced behaviors. The larvae of *Drosophila melanogaster* evacuate from their food, yeast paste, in response to hypoxia [41]. *Caenorhabditis elegans* migrates to an environment with a preferred oxygen availability to avoid hypoxia and hyperoxia [42, 43]. These behavioral responses are thought to be regulated by the nitric oxide (NO)/ cyclic guanosine monophosphate (cGMP) signaling pathway. In this pathway, soluble guanylyl cyclases play a key role in sensing oxygen *via* NO production [44, 45]. These cyclases produce cGMP in response to oxygen deprivation, and cGMP in turn activates cyclic nucleotide-gated ion channel (CNG). Activation of CNG allows calcium ions to pass through the plasma membrane, resulting in depolarization, which leads to the behavioral responses to hypoxia. Hypoxia-induced activation of TRPA1 homologue also increases calcium permeability. TRPA1 homologue as a hypoxia sensor may cooperate with sGC to promote escape from the sediment in hypoxic conditions.

The phylogenic analysis of the TRPA1 homologue gene suggested that the cloned TRPA gene from *C. teleta* was classified as a TRPAbasal gene, similar to nematode's TRPA-1 (Fig. 2-3). The known agonists of nematode's TRPA-1 are cold [46] and mechanical stimuli [35]. A starfish, *Patiria pectinifera*, has two TRPAs, TRPA1 and TRPA basal [36]. PpTRPA1 is thermosensitive and involved in thermotaxis, but PpTRPA basal is not activated by heat or several pungent chemicals. The oxygen dependent degradation domain is important for activation of TRPA1 by hypoxia. In the normoxic condition, a proline residue in the ODD is hydroxylated by the PHD family, which are oxygen-dependent prolyl hydroxylases [25]. Under hypoxic conditions, that proline is not hydroxylated, leading to activation of TRPA1. This oxygen-dependent

Fig. 2-6. Alignment of two CtTRPAbasal genes with ODDs in human HIFα
Alignment was performed using ClustalW. Jalview was used for analysis of this alignment. Coloring of amino acids was performed according to ClustalX. Arrowhead indicates hydroxylation site.

hydroxylation was first found in the regulation of HIFα, which mediates the physiological response to hypoxia [47]. Therefore, the ODDs from HIF-1α and 2α were aligned with CtTRPAbasal to examine whether CtTRPAbasal possesses an ODD (Fig. 2-4). The results of alignment showed that CtTRPAbasal has an ODD in the N-terminal cytosolic region, like mammalian TRPA1. This result suggested that CtTRPAbasal can be activated by hypoxia. On the other hand, online transcriptome data indicate the existence of a gene homologous to CtTRPAbasal, ELU03480.1, in *C. teleta*. This gene is also categorized into TRPAbasal (Fig. 2-3) but the proline residue in ODD is substituted by glutamine, which suggests that this gene is not involved in hypoxia detection (Fig. 2-6).

The whole-mount *in situ* hybridization analysis showed that *CtTRPAbasal* was transcribed precisely in the segment anterior to mouth called the prostomium (Fig. 2-5). In annelids, sensory cells for sensing environmental stimuli such as amino acids and pH are specifically localized in the prostomium [48-50]. Observation of the ventral view revealed that signals were observed in both sides of the prostomium. In the tip of the prostomium, nerve fibers are concentrated on both lateral sides [51]. Since the arrangement of nerve fibers is similar to the location of the *CtTRPAbasal* transcript signal there, CtTRPAbasal may function as a hypoxia sensor at the sensory cells in the prostomium. Therefore, *C.*

teleta might sense DO in its direction of movement and effectively avoid hypoxic zones. To specify more precisely the localization of CtTRPAbasal protein, immunohistochemical analyses will be needed.

A-967079 antagonizes mammalian TRPA1 with high specificity. Nakatsuka et al. (2013) and Banzawa et al. (2014) showed that A-967079 does not antagonize, but instead activates, chicken and frog TRPA1 [52, 53]. This difference of antagonistic or agonistic effects of A-967079 depends on several amino acids present in the 5th transmembrane region. The region containing these amino acids in CtTRPAbasal does not have high similarity with that in mammalian TRPA1. Therefore, there is a possibility that *C. teleta* has some other TRPA1 homologue with higher homology to mammalian TRPA1, and A-967079 has no antagonistic effect on CtTRPAbasal. On the other hand, CtTRPA1 contains an ODD, a key domain for hypoxia-activation, suggesting that CtTRPAbasal would regulate the hypoxia-induced response of *C. teleta*. The suppression of hypoxia-avoidance behavior of *C. teleta* by A-967079 supports the notion that A-967079 antagonizes CtTRPAbasal activation by hypoxia. Functional analyses of CtTRPAbasal itself will be needed to verify the hypoxia-sensing ability of CtTRPAbasal and the antagonistic effect of A-967079 on it.

To expand their habitats, it is important for organisms to sense the limit of their tolerance to physicochemical conditions for their survival. Organisms belonging to the *Capitella capitata* complex, including several capitellids of which *C. teleta* is one, can endure several days or more in severe hypoxic conditions [54]. *Capitella teleta* is thought to decrease its aerobic metabolism to below approximately 1.5 mg/L to endure hypoxic conditions, based on the results of its oxygen uptake rate [55]. These reports showed the high tolerance of *C. teleta* to hypoxia. In this study, *C. teleta* exhibited avoidance from severe hypoxia, possibly mediated by CtTRPAbasal, within one hour, and hence they could migrate to an area with higher DO before the time limit for their survival in severely hypoxic conditions. Their behavioral response and tolerance to hypoxia led them to survive in niches in organically enriched sediments where hypoxia often occurs. However, whether

CtTRPAbasal itself is activated by hypoxia needs to be clarified by loss-of-function methods or analysis of the ion channel function.

References

1. Breitburg D, Levin LA, Oschlies A, Grégoire M, Chavez FP, Conley DJ, et al. Declining oxygen in the global ocean and coastal waters. Science. 2018;359: eaam7240.
2. Diaz RJ, Rosenberg R. Spreading dead zones and consequences for marine ecosystems. Science. 2008;321: 926–929.
3. Keeling RF, Körtzinger A, Gruber N. Ocean deoxygenation in a warming world. Ann Rev Mar Sci. 2010;2: 199–229.
4. Vaquer-Sunyer R, Duarte CM. Thresholds of hypoxia for marine biodiversity. Proc Natl Acad Sci. 2008;105: 15452–15457.
5. Diaz RJ, Rosenberg R. Marine benthic hypoxia: A review of its ecological effects and the behavioural responses of benthic macrofauna. Oceanogr Mar Biol Ann Rev. 1995;33: 245–303.
6. Rosenberg, R. Benthic faunal recovery in a Swedish fjord following the closure of a sulphite pulp mill. OIKOS. 1972;23: 92-108.
7. Gray JS, Wu RSS, Or YY. Effects of hypoxia and organic enrichment on the coastal marine environment. Mar Ecol Prog Ser. 2002;238: 249–279.
8. Tsutsumi H. Population dynamics of *Capitella capitata* (Polychaeta; Capitellidae) in an organically polluted cove. Mar Ecol Prog Ser. 1987;36: 139–149.
9. Méndez N, Romero J, Flos J. Population dynamics and production of the polychaete *Capitella capitata* in the littoral zone of Barcelona (Spain, NW Mediterranean). J Exp Mar Bio Ecol. 1997;218: 263–284.
10. Wu RSS. Hypoxia: from molecular responses to ecosystem responses. Mar Pollut Bull. 2002;45: 35–45.

11. Gorr TA, Cahn JD, Yamagata H, Bunn HF. Hypoxia-induced synthesis of hemoglobin in the crustacean *Daphnia magna* is hypoxia-inducible factor-dependent. J Biol Chem. 2004;279: 36038–36047.
12. Albert JL, Ellington WR. Patterns of energy metabolism in the stone crab, *Menippe mercenaria*, during severe hypoxia and subsequent recovery. J Exp Zool. 1985;234: 175–183.
13. Sticle WB, Kapper MA, Liu LL, Gnaiger E, Wang SY. Metabolic adaptations of several species of crustaceans and molluscs to hypoxia: Tolerance and microcalorimetric studies. Biol Bull. 1989;177: 303–312.
14. Schöttler U, Grieshaber M. Adaptation of the polychaete worm *Scoloplos armiger* to hypoxic conditions. Mar Biol. 1988;99: 215–222.
15. Wang GL, Jiang BH, Rue EA, Semenza GL. Hypoxia-inducible factor 1 is a basic-helix-loop-helix-PAS heterodimer regulated by cellular O_2 tension. Proc Natl Acad Sci. 1995;92: 5510–5514.
16. Ke Q, Costa M. Hypoxia-inducible factor-1 (HIF-1). Mol Pharmacol. 2006;70: 1469–1480.
17. Gorr TA, Gassmann M, Wappner P. Sensing and responding to hypoxia via HIF in model invertebrates. J Insect Physiol. 2006;52: 349–364.
18. Kotsyuba EP. Hypoxia-inducible factor 1α in the central nervous system of the scallop *Mizuhopecten yessoensis* Jay, 1857 (Bivalvia: Pectinidae) during anoxia and elevated temperatures. Russ J Mar Biol. 2017;43: 293–301.
19. Piontkivska H, Chung JS, Ivanina AV, Sokolov EP, Techa S, Sokolova IM. Molecular characterization and mRNA expression of two key enzymes of hypoxia-sensing pathways in eastern oysters *Crassostrea virginica* (Gmelin): Hypoxia-inducible factor α (HIF-α) and HIF-prolyl hydroxylase (PHD). Comp Biochem Physiol Part D Genomics Proteomics. 2011;6: 103–114.
20. Li T, Brouwer M. Hypoxia-inducible factor, gsHIF, of the grass shrimp *Palaemonetes pugio*: Molecular characterization and response to hypoxia. Comp Biochem Physiol Part B Biochem Mol Biol. 2007;147: 11–19.

21. Soitamo AJ, Råbergh CMI, Gassmann M, Sistonen L, Nikinmaa M. Characterization of a hypoxia-inducible factor (HIF-1α) from rainbow trout. J Biol Chem. 2001;276: 19699–19705.
22. Wu RSS, Lam PKS, Wan KL. Tolerance to, and avoidance of, hypoxia by the penaeid shrimp (*Metapenaeus ensis*). Environ Pollut. 2002;118: 351–355.
23. Eby LA, Crowder LB. Hypoxia-based habitat compression in the Neuse River Estuary: context-dependent shifts in behavioral avoidance thresholds. Can J Fish Aquat Sci. 2002;59: 952–965.
24. Marshall DJ, McQuaid CD. Effects of hypoxia and hyposalinity on the heart beat of the intertidal limpets *Patella granvlaris* (Prosobranchia) and *Siphonaria capensis* (Pulmonata). Comp Biochem Physiol Part A Physiol. 1993;106: 65–68.
25. Takahashi N, Kuwaki T, Kiyonaka S, Numata T, Kozai D, Mizuno Y, et al. TRPA1 underlies a sensing mechanism for O_2. Nat Chem Biol. 2011;7: 701–711.
26. Pokorski M, Takeda K, Sato Y, Okada Y. The hypoxic ventilatory response and TRPA1 antagonism in conscious mice. Acta Physiol. 2014;210: 928–938.
27. Schneider CA, Rasband WS, Eliceiri KW. NIH Image to ImageJ: 25 years of image analysis. Nat Methods. 2012;9: 671–675.
28. Jones P, Binns D, Chang H-Y, Fraser M, Li W, McAnulla C, et al. InterProScan 5: genome-scale protein function classification. Bioinformatics. 2014;30: 1236–1240.
29. Kumar S, Stecher G, Tamura K. MEGA7: molecular evolutionary genetics analysis version 7.0 for bigger datasets. Mol Biol Evol. 2016;33: 1870–1874.
30. Finn RD, Coggill P, Eberhardt RY, Eddy SR, Mistry J, Mitchell AL, et al. The Pfam protein families database: towards a more sustainable future. Nucleic Acids Res. 2016;44: D279–D285.
31. Edgar RC. MUSCLE: multiple sequence alignment with high accuracy and high throughput. Nucleic Acids Res. 2004;32: 1792–1797.
32. Masson N, Willam C, Maxwell PH, Pugh CW, Ratcliffe PJ. Independent function of two destruction domains in hypoxia-inducible factor-α chains activated by prolyl hydroxylation. EMBO J. 2001;20: 5197–5206.

33. Larkin MA, Blackshields G, Brown NP, Chenna R, McGettigan PA, McWilliam H, et al. Clustal W and Clustal X version 2.0. Bioinformatics. 2007;23: 2947–2948.
34. Waterhouse AM, Procter JB, Martin DMA, Clamp M, Barton GJ. Jalview Version 2-a multiple sequence alignment editor and analysis workbench. Bioinformatics. 2009;25: 1189–1191.
35. Kindt KS, Viswanath V, Macpherson L, Quast K, Hu H, Patapoutian A, et al. *Caenorhabditis elegans* TRPA-1 functions in mechanosensation. Nat Neurosci. 2007;10: 568–577.
36. Saito S, Hamanaka G, Kawai N, Furukawa R, Gojobori J, Tominaga M, et al. Characterization of TRPA channels in the starfish *Patiria pectinifera*: involvement of thermally activated TRPA1 in thermotaxis in marine planktonic larvae. Sci Rep. 2017;7: 2173.
37. Hatano N, Itoh Y, Suzuki H, Muraki Y, Hayashi H, Onozaki K, et al. Hypoxia-inducible factor-1α (HIF1α) switches on transient receptor potential ankyrin repeat 1 (TRPA1) gene expression via a hypoxia response element-like motif to modulate cytokine release. J Biol Chem. 2012;287: 31962–31972.
38. Vismann B. Sulfide detoxification and tolerance in *Nereis (Hediste) diversicolor* and *Nereis (Neanthes) virens* (Annelida: Polychaeta). Mar Ecol Prog Ser. 1990;59: 229–238.
39. Llanso RJ, Diaz RJ. Tolerance to low dissolved oxygen by the tubicolous polychaete *Loimia medusa*. J Mar Biol Ass UK. 1994;74: 143–148.
40. Rosenberg R, Hellman B, Johansson B. Hypoxic tolerance of marine benthic fauna. Mar Ecol Prog Ser. 1991;79: 127–131.
41. Wingrove JA, O'Farrell PH. Nitric oxide contributes to behavioral, cellular, and developmental responses to low oxygen in *Drosophila*. Cell. 1999;98: 105–114.
42. Gray JM, Karow DS, Lu H, Chang AJ, Chang JS, Ellis RE, et al. Oxygen sensation and social feeding mediated by a *C. elegans* guanylate cyclase homologue. Nature. 2004;430: 317–322.

43. Chang AJ, Bargmann CI. Hypoxia and the HIF-1 transcriptional pathway reorganize a neuronal circuit for oxygen-dependent behavior in *Caenorhabditis elegans*. Proc Natl Acad Sci. 2008;105: 7321–7326.
44. Morton DB. Atypical soluble guanylyl cyclases in *Drosophila* can function as molecular oxygen sensors. J Biol Chem. 2004;279: 50651–50653.
45. Vermehren-Schmaedick A, Ainsley JA, Johnson WA, Davies S-A, Morton DB. Behavioral responses to hypoxia in *Drosophila* larvae are mediated by atypical soluble guanylyl cyclases. Genetics. 2010;186: 183–196.
46. Xiao R, Zhang B, Dong Y, Gong J, Xu T, Liu J, et al. A genetic program promotes *C. elegans* longevity at cold temperatures via a thermosensitive TRP channel. Cell. 2013;152: 806–817.
47. Kaelin WG, Ratcliffe PJ. Oxygen sensing by metazoans: the central role of the HIF hydroxylase pathway. Mol Cell. 2008;30: 393–402.
48. Lindsay SM, Riordan TJ, Forest D. Identification and activity-dependent labeling of peripheral sensory structures on a spionid polychaete. Biol Bull. 2004;206: 65–77.
49. Laverack MS. Tactile and chemical perception in earthworms –I. Responses to touch, sodium chloride, quinine and sugars. Comp Biochem Physiol. 1960;1: 155–163.
50. Laverack MS. Tactile and chemical perception in earthworms –II. Responses to acid pH solutions. Comp Biochem Physiol. 1961;2: 22–34.
51. Meyer NP, Carrillo-Baltodano A, Moore RE, Seaver EC. Nervous system development in lecithotrophic larval and juvenile stages of the annelid *Capitella teleta*. Front Zool. 2015;12: 15.
52. Nakatsuka K, Gupta R, Saito S, Banzawa N, Takahashi K, Tominaga M, et al. Identification of molecular determinants for a potent mammalian TRPA1 antagonist by utilizing species differences. J Mol Neurosci. 2013;51: 754–762.
53. Banzawa N, Saito S, Imagawa T, Kashio M, Takahashi K, Tominaga M, et al. Molecular basis determining inhibition/activation of nociceptive receptor TRPA1 protein. J Biol Chem. 2014;289: 31927–31939.

54. Warren LM. The ecology of *Capitella capitata* in British waters. J Mar Biol Ass UK. 1977;57: 151–159.
55. Chareonpanich C, Montani S, Tsutsumi H, Nakamura H. Estimation of oxygen consumption of a deposit-feeding polychaete *Capitella* sp. I. Fish Sci. 1994;60: 249–251.

Chapter 3

Transcriptomic analyses reveal hypoxia-inducing responses in marine annelid, *Capitella teleta.*

Introduction

In previous chapter, I demonstrated that the hypoxia-escaping behavior of *C. teleta*, however, the mechanism that they can survive even in hypoxic condition remains unclear. Marine annelids have relatively high tolerance to hypoxia among marine invertebrates since they are capable of withstanding hypoxia for several days [1-3]. Marine annelids improve their tolerance to chronic hypoxia in various ways. Morphological changes to expand surface contact with environmental water are reported in Spionidae species living in oxygen minimum zone [4]. The empowerments of energy productivity by increasing the number of pyruvate oxidoreductase involving anaerobic metabolism also play a key role for the adaptation on hypoxic conditions [5]. To survive longer in hypoxia, marine annelids ameliorate oxygen acquirements by rise in hemoglobin concentration [6] and gain energy from anaerobic metabolism [7-9]. However, there is little knowledge about the molecular basis of these responses.

Recent advances in genomic and transcriptomic analysis are revealing molecular basis of hypoxia-inducing responses of marine invertebrates, especially fishery important species such as river prawn [10, 11], pacific oyster [12] and sea cucumber [13]. There is quite a few study about transcriptomic response to deprivation of oxygen in marine annelids. In 2012, the draft genomic sequence of *C. teleta* became available [14]. This advance helps us to understand the response of marine annelids to environmental stresses. In this chapter, to reveal the molecular basis supporting their adaptability to hypoxic condition, RNA-seq analysis were conducted. Here, I showed that *C. teleta* scavenges oxidative stress produced by hypoxia and reoxygenation and changes the set of globin genes to optimize oxygen availability in hypoxic condition in response to hypoxia.

Materials and Methods

Rearing of *Capitella teleta*

Stock cultures of *C. teleta* were kindly spared from Dr. Hiroaki Tsutsumi and Dr. Naoko Ueda, and reared in the mud with the artificial sea water (ASW) (Rei-sea marine II, Iwaki, Tokyo, Japan) of 33 psu salinity at 18°C The worms were originally collected at the sediment below the fish farm (32°23’52 N, 130°13’40 E) or Dokai Bay (33°52’34 N, 130°45’3 E). Worms were fed with commercial fish food.

Hypoxia challenge

After worms were relaxed in half mixture of ASW and 0.37 M $MgCl_2$, worms with 0.4-0.6 cm in length were collected as “Small” and female worms with more than 1.2 cm in length as “Large”. Recovering from relaxing by soaked in ASW for 1 h, worms were transferred into reagent bottle filled with hypoxic ASW or normoxic one and the caps were closed tightly. The volume capacity of this bottle is nearly 250 mL. Dissolved oxygen concentration in hypoxia was set roughly at 1 mg/L (precisely 0.88 mg /L). Hypoxia was achieved by blowing N_2 gas. In normoxia, DO was set more than 6 mg/L. Dissolved oxygen concentrations were measured with InLab OptiOx connected to Seven 2 GO Pro (METTLER TOLEDO, Columbus, USA). The worms within the bottle were kept for 24 h at 18°C.

RNA extraction and RNA-seq

Total RNA of samples were extracted from whole-body of the worms by using RNeasy Mini Kit (QIAGEN, Hilden, Germany) with the option of on-column digestion of genomic DNA. Five small worms were pooled into one sample as small group, because total RNA amount from one small worm was not enough for RNA-seq analysis. Libraries were constructed by TruSeq RNA Sample Prep Kit v2 (Illumina, CA, USA) following the protocol TruSeq RNA Sample Preparation v2 Guide, Part # 15026495 Rev. F. 100 bp, pair end sequencing were done with NovaSeq 6000 (Illumina). Library construction and RNA sequencing were performed at Macrogen (Seoul, South Korea).

Data analysis

The quality of the sequences was checked and the sequence reads with Phred quality score < 20, length < 80 bp were trimmed by TrimGalore!-0.45 (https://github.com/FelixKrueger/TrimGalore). The adaptor sequence was also trimmed by TrimGalore!-0.45. The trimmed sequences were mapped to transcripts of *C. teleta* deposited in Ensembl Metazoa (https://metazoa.ensembl.org/index.html) then quantified with Salmon v0.11.4 [15]. The quantified data sets were exported by tximport 1.8.0 [16]. The exported data sets were imported to R 3.5.1 and analyzed as follows. The imported data was normalized by iDEGS/edgeR methods in TCC 1.20.1 package [17]. Normalization was separately done in two groups: Large normoxia and Large hypoxia, Small normoxia and Small hypoxia. Differentially expressed genes (DEGs) were defined as a.value > 0, m.value > 1 or < -1, q.value < 0.05. The list of Gene IDs, GO term and GO description were acquired Ensembl Metazoa Biomart. The enriched GO were statistically determined by Fisher's exact test. Annotation of DEGs were done with Blast2GO 5.2.5 [18]. The *E*-value cutoff was set as 1.0E-5 and gene description was determined by BLAST Description Annotator in Blast2GO.

Phylogenic analysis of globin genes

The amino acid sequences of globin genes were acquired from Ensembl Metazoa Biomart. These globin genes were annotated by Blast2GO and two sequences (Table 3-6) CapteG189648 and CapteG60954 were omitted in this analysis because CapteG189648 was not annotated and CapteG60954 have high similarity to flavohemoprotein, which is involved in NO detoxification. These sequences and the amino acid sequences of known annelid globins, crustacean neuroglobin and cytoglobin, pacific oyster neuroglobin, and vertebrates' glonbins listed in Table 3-1 were aligned with MUCLE in MEGA7 [19]. The site under 80% coverage were trimmed. The number of sites used in phylogenic analysis was 134. The best model estimation was carried out in MEGA7. The trimmed alignment data were exported as nexus format. Then, Bayesian tree was generated from 2×10^6 generation with 4 chains in MrBayes 3.2.6 [20], estimating posterior probability from Markov chain Monte Carlo method. The LG + G model was applied to this analysis.

Table 3-1. The list of globin genes used for phylogenic analysis

Name in tree	Accession	Species	Name in tree	Accession	Species
Aa_NMb	Q93101	*Aphrodite aculeata*	Hs_Cb	NP_599030.1	*Homo sapiens*
Am_HbA2	Q53I65	*Arenicola marina*	Hs_HbA	P69905.2	*Homo sapiens*
Am_HbB2	Q53I64	*Arenicola marina*	Hs_HbB	P68871.2	*Homo sapiens*
Ap_HbInt	Q53I62	*Alvinella pompejana*	Hs_Mb	NP_001349775.1	*Homo sapiens*
Bc_Hb1	ADO63770.1	*Branchiplicatus cupreus*	Hs_Nb	NP_067080.1	*Homo sapiens*
Bc_Hb2	ADO63771.1	*Branchiplicatus cupreus*	Lsp_GB1	Q7Z1R4	*Lamellibrachia* sp.
Bns_Hb	ADO63769.1	*Branchinotogluma segonzaci*	Lsp_HbAIII	P15469.1	*Lamellibrachia* sp.
Bnt_Hb	ADO63768.1	*Branchinotogluma trifurcus*	Lsp_HbB2	Q86BV3	*Lamellibrachia* sp.
Bpse_Gex1	ACU21600.1	*Branchipolynoe seepensis*	Lt_GEx1	P08924.1	*Lumbricus terrestris*
Bpse_Gex2	ACU21601.1	*Branchipolynoe seepensis*	Lt_GEx2	P02218.2	*Lumbricus terrestris*
Bpse_Gex3	ACU21602.1	*Branchipolynoe seepensis*	Lt_GEx3	P11069.3	*Lumbricus terrestris*
Bpse_Gex4	ACU21603.1	*Branchipolynoe seepensis*	Lt_GEx4	P13579.1	*Lumbricus terrestris*
Bpse_Gex5	ACU21605.1	*Branchipolynoe seepensis*	Lt_Hbd2	AAC14536.1	*Lumbricus terrestris*
Bpsy_Gex1	ACU21596.1	*Branchipolynoe symmytilida*	Lw_Hb	ADO63772.1	*Lepidonotopodium williamsae*
Bpsy_Gex2	ACU21597.1	*Branchipolynoe symmytilida*	Ob_Mb	Q56JK7	*Ophelia bicornis*
Bpsy_Gex3	ACU21598.1	*Branchipolynoe symmytilida*	Pv_Cb	ASN74468.1	*Penaeus vannamei*
Bpsy_Gex4	ACU21599.1	*Branchipolynoe symmytilida*	Rp_HbA1	Q8IFK4	*Riftia pachyptila*
Bpsy_Gex5	ACU21604.1	*Branchipolynoe symmytilida*	Rp_HbB	P80592.1	*Riftia pachyptila*
Cg_Nb1	EKC29694.1	*Crassostrea gigas*	Rp_HbB1b	Q8IFK1	*Riftia pachyptila*
Cg_Nb2	EKC32095.1	*Crassostrea gigas*	Rp_HbB2	Q8IFJ9	*Riftia pachyptila*
Cg_Nb3	EKC33472.1	*Crassostrea gigas*	Ss_G	Q9BHK3	*Sabella spallanzanii*
Dm_Nb1	KZS06152.1	*Daphnia magna*	Ss_G2	CAC37411.1	*Sabella spallanzanii*
Dm_Nb2	KZS17126.1	*Daphnia magna*	Ss_G3	Q9BHK1	*Sabella spallanzanii*
Dm_Nb3	KZS21721.1	*Daphnia magna*	Th_GEx1	P02219.1	*Tylorrhynchus heterochaetus*
Dr_Cb	NP_694484.1	*Danio rerio*	Th_GEx2A	P09966.1	*Tylorrhynchus heterochaetus*
Dr_GX	CAG25723.1	*Danio rerio*	Th_GEx2B	P13578.1	*Tylorrhynchus heterochaetus*
Dr_HbA	NP_571332.3	*Danio rerio*	Th_GEx2C	P02220.1	*Tylorrhynchus heterochaetus*
Dr_HbB	NP_571095.1	*Danio rerio*	Tt_GEx	P18202.1	*Tubifex tubifex*
Dr_Mb	NP_001349318.1	*Danio rerio*	Uc_HbA	1ITH_A	*Urechis caupo*
Dr_Nb	NP_571928.1	*Danio rerio*	Uc_HbB	1ITH_B	*Urechis caupo*
Ev_HbA1	Q9BKE9	*Eudistylia vancouveri*	Uu_Hb	AIN56733.1	*Urechis unicinctus*
Gd_G	P02216.2	*Glycera dibranchiata*	Xt_Cb	AAH76983.1	*Xenopus tropicalis*
Gd_GP1	P23216.1	*Glycera dibranchiata*	Xt_GX	CAG25551.1	*Xenopus tropicalis*
Gd_GP2	AAA29160.1	*Glycera dibranchiata*	Xt_HbA	NP_988860.1	*Xenopus tropicalis*
Gd_GP3	AAA29161.1	*Glycera dibranchiata*	Xt_HbB	NP_988859.1	*Xenopus tropicalis*
Gg_Cb	NP_001008789.1	*Gallus gallus*	Xt_Nb	AAI61728.1	*Xenopus tropicalis*
Gg_HbA	NP_001004376.1	*Danio rerio*			
Gg_HbB	NP_990820.1	*Gallus gallus*			
Gg_Mb	NP_001161224.1	*Gallus gallus*			
Gg_Nb	CAG25721.1	*Gallus gallus*			

Trees were sampled in each 100 and the value of burn-in was set to 2×10^5. The average standard deviation of split frequencies was 0.00979.

Clustering analysis of globin genes

Quantified transcripts data of all groups from Salmon were normalized by iDEGS/edgeR methods in TCC package. The normalized data sets of globins were extracted and z-scored by genefileter 1.62.0. Then, heatmap was constructed by

ComplexHeatmap 1.18.1 [21]. Clustering of the globin genes was done using Ward's method with Euclidean distance. The globin genes were divided into 4 clusters.

Results

Sequencing and alignment results

RNA-seq produced 4,120,235,410 bp - 5,482,101,634 bp with 40,794,410 - 54,278,234 reads (Table 3-2). The sequences trimmed by TrimGalore! was 0.22% - 0.27% of all sequences. The 70.38 - 72.88% trimmed sequences were successfully mapped to cDNA library of *C. teleta* by Salmon.

To know the hypoxia-inducing response of *C. teleta*, differentially expressed genes in response to hypoxia were estimated in both large and small groups. The number of DEGs were 938 in large group and 769 in small group (Fig. 3-1). The number of commonly upregulated genes in both groups were 299 genes. The number of upregulated genes specific in large group were 376, while that in small group were 251. 57 genes were commonly downregulated in the both, 205 were specific to large group and 162 were specific to small group. The highly upregulated genes in both groups by hypoxia were heat shock proteins (Tables 3-3 and 3-4). Some globin genes were highly upregulated but other ones highly downregulated in small groups. In large group, only downregulation of some globin genes was prominent, while some globins were slightly upregulated.

Gene Ontology enrichment analysis

To speculate the functional responses to hypoxia of *C. teleta*, gene ontology enrichment analysis was conducted (Table 3-5). Hypoxia treatment altered the frequency of GO involving oxygen uptake and storage, such as GO:0005344, oxygen carrier activity; GO:0019825, oxygen binding; GO:0020037, heme binding. GO:0004867, serine-type endopeptidase inhibitor activity was also enriched in both groups.

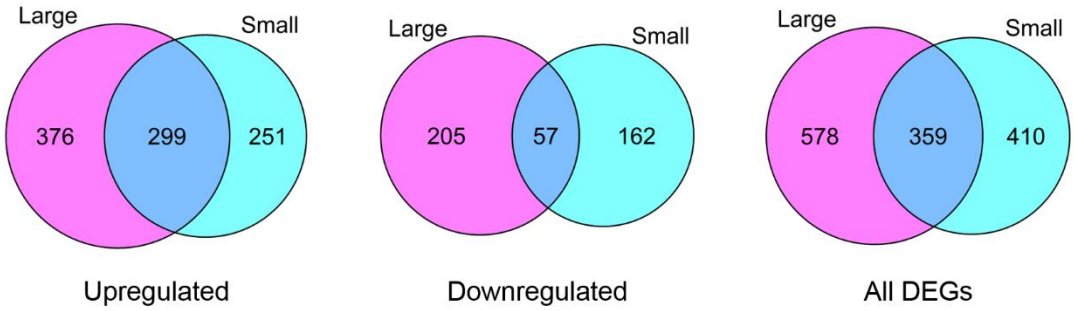

Fig. 3-1. Venn diagram of differentially expressed genes (DEGs) by hypoxia
DEGs were filtered with the threshold as follows, A-value > 1; M-value <-1 (down regulate) or >1 (upregulate); *q*-value < 0.05.

Table 3-2. Summary of sequencing and alignment

Group	Treatment	Sample	Total read bases (bp)	Total reads	Q20(%)	Trimmed reads	Mapping rate (%)
Large	Normoxia	LN1	4,486,185,882	44,417,682	98.36	50,572 (0.23%)	72.88
		LN2	4,713,469,010	46,668,010	98.42	53,038 (0.23%)	71.60
		LN3	5,056,371,484	50,063,084	98.42	63,505 (0.25%)	71.03
	Hypoxia	LH1	4,395,127,918	43,516,118	98.21	53,858 (0.25%)	72.68
		LH2	4,120,235,410	40,794,410	98.41	52,973 (0.26%)	72.46
		LH3	4,343,131,502	43,001,302	98.42	57,621 (0.27%)	70.38
Small	Normoxia	SN1	4,988,795,414	49,394,014	98.34	59,439 (0.24%)	71.32
		SN2	4,495,985,912	44,514,712	98.37	54,048 (0.24%)	71.32
		SN3	5,220,889,576	51,691,976	98.47	64,699 (0.25%)	70.94
	Hypoxia	SH1	4,870,404,426	48,221,826	98.31	53,730 (0.22%)	72.35
		SH2	5,482,101,634	54,278,234	98.51	64,930 (0.24%)	71.11
		SH3	4,782,130,628	47,347,828	98.20	61,404 (0.26%)	71.61

Table 3-3. The list of genes with highly differential expression by hypoxia in large group

Up- or Down-regulation	Gene ID	Description	*E*-value	A-value	M-value	*q*-value
Up	CapteG220370	vascular endothelial growth factor A-like isoform X1	1.9E-32	5.58	9.03	9.9.E-04
	CapteG31498	tetraspanin-7-like	3.1E-39	3.93	8.60	7.1.E-31
	CapteG139354	sushi, von Willebrand factor type A, EGF and pentraxin domain-containing protein 1-like	1.2E-25	3.81	6.58	8.9.E-11
	CapteG219425	Protein lethal(2)essential for life	3.9E-08	8.21	6.55	5.1.E-08
	CapteG21898	Heat shock protein 70 B2	0.0E+00	7.31	6.38	1.2.E-31
	CapteG155585	heat shock protein 70	0.0E+00	8.00	6.30	6.0.E-39
	CapteG149823	heat shock protein 70 B2-like	0.0E+00	5.73	5.98	1.9.E-28
	CapteG70307	putative prestalk protein	8.0E-16	4.69	5.51	2.6.E-05
	CapteG124063	DNA-dependent protein kinase catalytic subunit-like	1.0E-63	4.35	5.44	4.6.E-03
	CapteG190767	cyclic GMP-AMP synthase-like	1.2E-14	3.35	5.31	5.4.E-03
	CapteG189456	membrane-spanning 4-domains subfamily A member 8	1.0E-09	5.63	5.31	3.6.E-08
	CapteG209914	metalloreductase STEAP4-like	6.3E-76	3.40	5.18	4.4.E-03
	CapteG186607	DEAD-domain-containing protein	0.0E+00	8.47	5.17	1.1.E-15
	CapteG196425	gamma-aminobutyric acid type B receptor subunit 2-like	8.4E-99	3.06	5.01	9.6.E-03
	CapteG68267	macrophage mannose receptor 1-like	6.5E-22	4.64	4.97	5.9.E-10
	CapteG145065	THAP domain-containing protein 1	5.2E-35	4.22	4.94	6.9.E-03
	CapteG208459	vitellogenin	8.7E-82	5.79	4.86	1.1.E-02
	CapteG210159	sushi, von Willebrand factor type A, EGF and pentraxin domain-containing protein 1	7.5E-159	9.95	4.82	1.8.E-10
	CapteG33454	beta-1,3-glucan-binding protein precursor	7.0E-89	2.33	4.74	5.0.E-02
	CapteG114926	arylsulfatase F	2.4E-34	3.25	4.74	4.1.E-03
Down	CapteG119820	Elongation factor 1-beta	9.3E-47	6.02	-11.51	2.7.E-03
	CapteG201276	extended synaptotagmin-2-like isoform X3	1.9E-14	4.66	-8.26	1.3.E-28
	CapteG1218	globin	6.8E-24	8.59	-7.83	3.1.E-16
	CapteG198414	keratin-associated protein 6-2-like	1.3E-08	5.30	-7.35	4.1.E-02
	CapteG202092	keratin-associated protein 6-2-like	1.9E-08	6.25	-7.15	1.2.E-02
	CapteG975	globin	6.8E-24	7.72	-6.96	3.0.E-04
	CapteG817	globin	6.8E-24	13.53	-6.68	2.2.E-15
	CapteG44392	atrial natriuretic peptide receptor 1	6.6E-86	2.75	-6.54	7.8.E-04
	CapteG201785	ankyrin repeat protein	4.1E-18	3.28	-6.42	4.2.E-03
	CapteG141748	IgGFc-binding protein-like	1.3E-35	6.86	-6.40	4.3.E-02
	CapteG201296	transcriptional regulatory protein LGE1	3.3E-08	5.79	-6.40	1.7.E-02
	CapteG201297	transcriptional regulatory protein LGE1	2.7E-08	6.03	-6.05	1.0.E-02
	CapteG3904	transcriptional regulatory protein LGE1	4.0E-08	7.09	-5.91	8.4.E-04
	CapteG225826	globin	3.7E-24	9.43	-5.81	1.4.E-07
	CapteG144205	dehydrogenase/reductase SDR family member 4	3.6E-70	1.60	-5.35	1.1.E-02
	CapteG201337	No mechanoreceptor potential A	4.1E-16	4.44	-5.23	2.8.E-02
	CapteG216869	flavin-containing monooxygenase FMO GS-OX-like 8	2.3E-147	8.32	-5.08	2.1.E-07
	CapteG163545	60S ribosomal protein L18a	8.5E-54	7.74	-5.03	1.3.E-02
	CapteG213062	flavin-containing monooxygenase FMO GS-OX-like 8	4.2E-65	6.20	-4.97	1.2.E-14
	CapteG143890	piwi-like protein 1 isoform X1	8.3E-113	5.00	-4.90	1.1.E-02

The top 20 DEGs successfully annotated are shown. The *E*-value is a parameter indicating the probability one can annotate the description by chance. A-value is $\log_2$ scaled average expression level. M-value is $\log_2$ scaled fold-change of the expression level in hypoxia compared to normoxia. *q*-value is false discovery rate.

Table 3-4. The list of genes with highly differential expression by hypoxia in small group

Up- or Down-regulation	Gene ID	Description	*E*-value	A-value	M-value	*q*-value
Up	CapteG21898	Heat shock protein 70 B2	0.0.E+00	8.00	6.39	1.8.E-62
	CapteG132766	F-I hemoglobin	1.2.E-26	9.62	6.32	7.7.E-18
	CapteG155585	heat shock protein 70	0.0.E+00	8.75	6.12	9.8.E-63
	CapteG149823	heat shock protein 70 B2-like	0.0.E+00	6.74	6.03	3.1.E-65
	CapteG192931	F-I hemoglobin	1.4.E-26	11.42	5.37	5.9.E-33
	CapteG225294	Protein lethal(2)essential for life	6.3.E-09	10.52	4.55	6.1.E-73
	CapteG103071	heat shock 70 kDa protein 1-like	1.1.E-65	5.25	4.49	7.8.E-05
	CapteG128650	histone H4-like	7.9.E-51	5.93	4.34	6.6.E-07
	CapteG219425	Protein lethal(2)essential for life	3.9.E-08	9.30	4.22	1.2.E-44
	CapteG225284	Protein lethal(2)essential for life	2.7.E-08	9.45	4.16	4.4.E-55
	CapteG75410	EGF-like repeat and discoidin I-like domain-containing protein 3 isoform X1	5.9.E-19	3.30	4.10	5.7.E-03
	CapteG191632	reverse transcriptase-like protein	3.1.E-20	1.70	3.83	1.4.E-02
	CapteG157638	histone H4-like	7.9.E-51	3.55	3.82	5.8.E-03
	CapteG133846	steroid 17-alpha-hydroxylase/17,20 lyase-like	3.7.E-66	8.50	3.75	1.8.E-41
	CapteG122794	alternative oxidase, mitochondrial-like	8.6.E-126	9.33	3.71	1.2.E-66
	CapteG134085	RNA-directed DNA polymerase from mobile element jockey	6.9.E-10	3.78	3.64	2.1.E-02
	CapteG198869	histone H2A	6.8.E-117	3.84	3.63	1.3.E-02
	CapteG103539	histone H4-like	7.9.E-51	3.10	3.62	4.8.E-02
	CapteG227551	alternative oxidase, mitochondrial-like	1.1.E-125	7.60	3.57	5.5.E-40
	CapteG39548	sushi, von Willebrand factor type A, EGF and pentraxin domain-containing protein 1-like	3.9.E-28	7.78	3.46	3.9.E-12
Down	CapteG1218	globin	6.8.E-24	8.79	-5.98	5.8.E-11
	CapteG817	globin	6.8.E-24	13.35	-4.99	7.4.E-12
	CapteG107496	predicted protein	3.1.E-17	1.49	-4.76	5.5.E-03
	CapteG217153	Down syndrome cell adhesion molecule	1.9.E-17	3.05	-4.64	1.9.E-04
	CapteG81459	acetyl-CoA acetyltransferase, cytosolic-like	5.4.E-70	2.77	-4.26	3.3.E-04
	CapteG133647	epsin-1-like isoform X1	4.4.E-08	4.73	-4.18	7.9.E-04
	CapteG35564	UDP-glucuronosyltransferase 2C1-like	5.6.E-66	3.16	-3.89	1.5.E-03
	CapteG163794	molybdenum cofactor biosynthesis protein 1 isoform X1	4.8.E-63	2.44	-3.87	2.9.E-02
	CapteG214864	C-type lectin domain family 17, member A-like	5.5.E-10	2.59	-3.74	7.8.E-03
	CapteG218142	Proteophosphoglycan ppg4	2.9.E-36	4.24	-3.49	2.1.E-02
	CapteG975	globin	6.8.E-24	6.38	-3.45	8.7.E-03
	CapteG143106	dehydrogenase/reductase SDR family member 7-like	1.0.E-117	4.78	-3.36	3.2.E-05
	CapteG5577	2-hydroxyacylsphingosine 1-beta-galactosyltransferase-like isoform X2	1.9.E-106	7.20	-3.03	5.9.E-10
	CapteG138513	beta-1,3-galactosyltransferase 1-like	8.4.E-62	3.31	-3.00	1.5.E-02
	CapteG104502	probable indole-3-acetic acid-amido synthetase GH3.9 isoform X1	1.8.E-85	6.99	-2.90	9.8.E-12
	CapteG81520	zinc finger BED domain-containing protein 1-like	5.3.E-17	5.10	-2.79	1.7.E-02
	CapteG114418	steroid 17-alpha-hydroxylase/17,20 lyase-like	1.5.E-89	7.52	-2.79	3.2.E-16
	CapteG219444	bactericidal permeability increasing protein	1.3.E-25	5.83	-2.76	7.8.E-04
	CapteG210871	fibrinogen C domain-containing protein 1-like	4.3.E-09	10.75	-2.69	7.2.E-19
	CapteG134544	solute carrier family 13 member 2	5.6.E-130	6.38	-2.60	2.6.E-09

The top 20 DEGs successfully annotated are shown. The *E*-value is a parameter indicating the probability one can annotate the description by chance. A-value is $\log_2$ scaled average expression level. M-value is $\log_2$ scaled fold-change of the expression level in hypoxia compared to normoxia. *q*-value is false discovery rate.

Table 3-5. Gene ontology enrichment analysis

Group	GO term accession	GO term name	Number of DEGs	Total in category	*p*-value
Large	GO:0004857	enzyme inhibitor activity	14	31	9.3E-09
	GO:0004867	serine-type endopeptidase inhibitor activity	18	72	1.5E-07
	GO:0005344	oxygen carrier activity	12	48	1.8E-05
	GO:0019825	oxygen binding	12	48	1.8E-05
	GO:0020037	heme binding	28	230	3.5E-05
Small	GO:0020037	heme binding	33	230	2.8E-09
	GO:0016705	oxidoreductase activity, acting on paired donors, with incorporation or reduction of molecular oxygen	23	142	1.0E-07
	GO:0005506	iron ion binding	26	181	1.3E-07
	GO:0004497	monooxygenase activity	19	104	2.6E-07
	GO:0004857	enzyme inhibitor activity	11	31	3.9E-07
	GO:0004867	serine-type endopeptidase inhibitor activity	15	72	1.1E-06
	GO:0005344	oxygen carrier activity	10	48	6.9E-05
	GO:0019825	oxygen binding	10	48	6.9E-05
	GO:0055114	oxidation-reduction process	53	734	9.4E-05

p-value is the probability for Fisher's exact test. The GO category with *p*-value < 1.0E-0.4 are shown in this table.

Expression pattern and phylogeny for globins

To examine the response in globin genes to hypoxia, the unrooted Bayesian tree of globin genes including that among annelids and other taxa was constructed (Fig. 3-3). All globin genes of *C. teleta* were located at the clade of intracellular globins. Their globin genes are divided into two clades, one is the clade containing vertebrates' neuroglobin and globin X, and metazoan neuroglobin, the another is that containing annelid intracellular globin and red blood cell hemoglobin from *Urechis caupo*. Polynoidae extracellular globin genes are located at the same clade as annelid intracellular globin genes. This phylogeny was the same as the report in Projecto-Garcia et al. (2017) [22]. Heatmap analysis implied the rule of expression according to the growth stage and DO level (Fig. 3-2). The globin genes in cluster 1 showed relatively high expression in large worms during normoxia and downregulated by hypoxia. Cluster 2 genes seems to be upregulated by hypoxia in both growth stages. The genes in cluster 4 were relatively high expression in small worms and

Table 3-6. The annotation of globin genes in *Capitella teleta*

Gene ID	Description	*E*-value	Up- or Down- regulation	
			Large	Small
CapteG110047	hemoglobin subunit mu-like	6.63E-53		
CapteG114226	F-I hemoglobin	2.76E-19		
CapteG1218	globin	6.79E-24	Down	Down
CapteG132766	F-I hemoglobin	1.19E-26	Up	Up
CapteG144794	cytoglobin-2-like isoform X1	1.32E-24		
CapteG1470	F-I hemoglobin	1.28E-25	Down	
CapteG147415	neuroglobin-like isoform X2	3.12E-29		
CapteG158355	F-I hemoglobin	3.27E-26		Up
CapteG166020	non-symbiotic hemoglobin 1-like isoform X1	2.82E-38		
CapteG166267	F-I hemoglobin	1.20E-27		Up
CapteG170177	F-I hemoglobin	1.64E-15		Up
CapteG181579	globin D, coelomic-like	2.05E-27		
CapteG18433	hemoglobin	1.16E-24		
CapteG184905	F-I hemoglobin	1.20E-27		
CapteG188542	non-symbiotic hemoglobin 1-like	8.20E-47		
CapteG188798	hemoglobin subunit mu-like	5.11E-17		
CapteG189648	---NA---			
CapteG190593	hemoglobin subunit mu-like	1.75E-32		
CapteG192439	neuroglobin-like	5.07E-24		
CapteG192931	F-I hemoglobin	1.36E-26	Up	Up
CapteG193618	neuroglobin isoform X1	1.74E-20		
CapteG194549	Neuroglobin	7.80E-21		
CapteG195701	hemoglobin subunit mu-like	8.53E-17		
CapteG198978	hemoglobin subunit mu-like	3.40E-35		
CapteG200756	cytoglobin-2 isoform X1	1.04E-17		
CapteG20182	F-I hemoglobin	3.16E-18	Up	Up
CapteG21023	F-I hemoglobin	1.98E-27		
CapteG21094	F-I hemoglobin	1.30E-27		
CapteG214116	neuroglobin-like isoform X3	2.55E-43		
CapteG21508	F-I hemoglobin	5.48E-27		
CapteG216611	F-I hemoglobin	1.13E-26	Down	
CapteG218767	globin D, coelomic-like	1.17E-26		
CapteG219237	F-I hemoglobin	1.48E-21		
CapteG21927	F-I hemoglobin	2.77E-24		
CapteG219905	F-I hemoglobin	1.38E-24	Down	Down
CapteG221680	F-I hemoglobin	2.02E-26		
CapteG225570	F-I hemoglobin	2.52E-26	Down	
CapteG225826	globin	3.70E-24	Down	
CapteG227018	neuroglobin-like	1.58E-30		
CapteG227604	F-I hemoglobin	2.74E-25		
CapteG229341	hemoglobin chain	4.83E-25		
CapteG27881	neuroglobin-like	1.20E-25		
CapteG5226	globin-like	2.84E-18		
CapteG5378	F-I hemoglobin	1.88E-26	Down	
CapteG60954	NO-inducible flavohemoprotein	2.25E-104		
CapteG817	globin	6.79E-24	Down	Down
CapteG975	globin	6.79E-24	Down	Down
CapteG98019	hemoglobin subunit mu-like	5.09E-56		

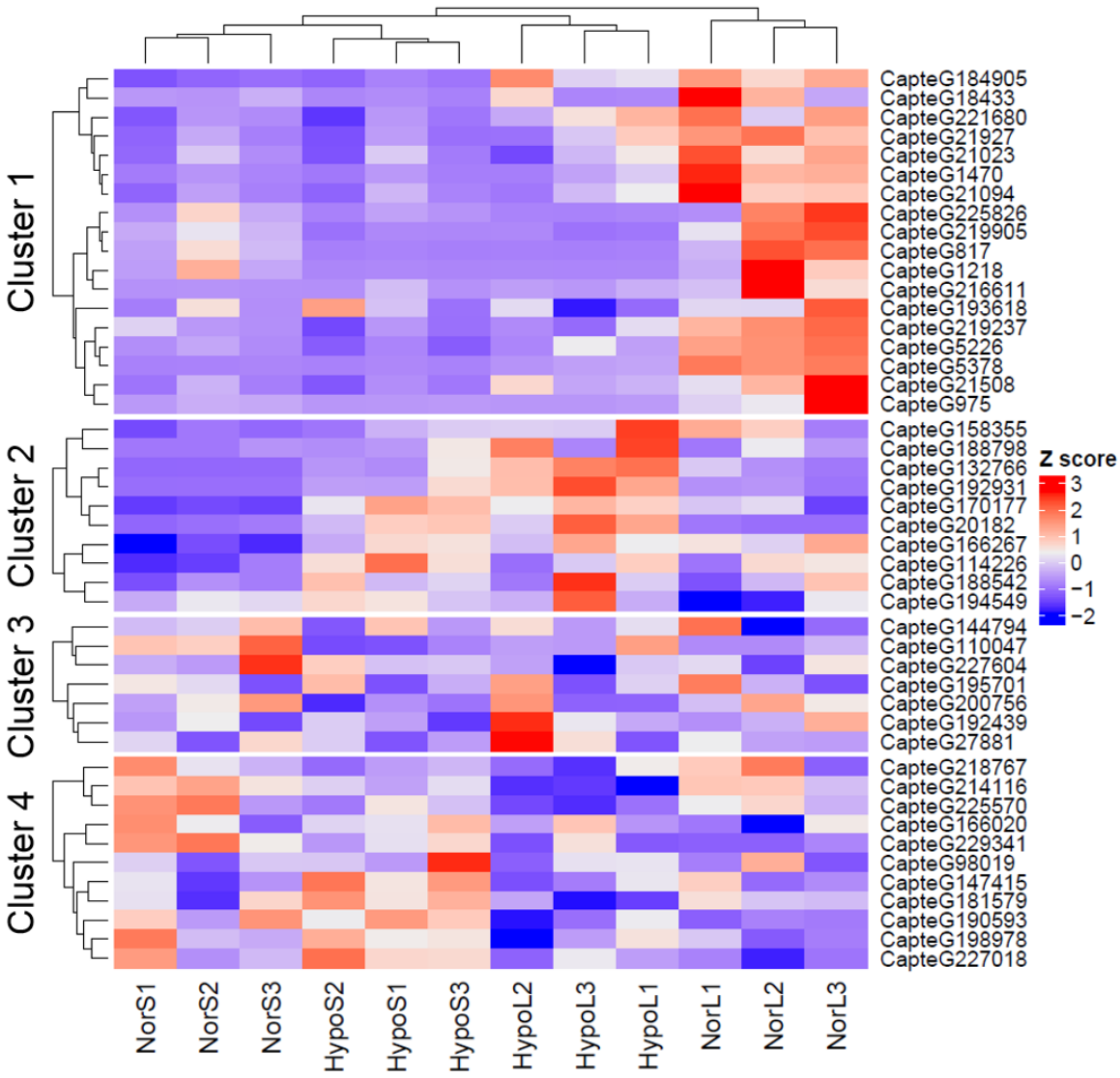

Fig. 3-2. Clustering analysis of globin genes

Clustering analysis of globin genes was done by the Ward's method with Euclidian distances between z-scored expression levels of each genes. The heatmap was depicted by R 3.5.1. Red cell indicates relatively high expression level and blue cell does relatively low expression level.

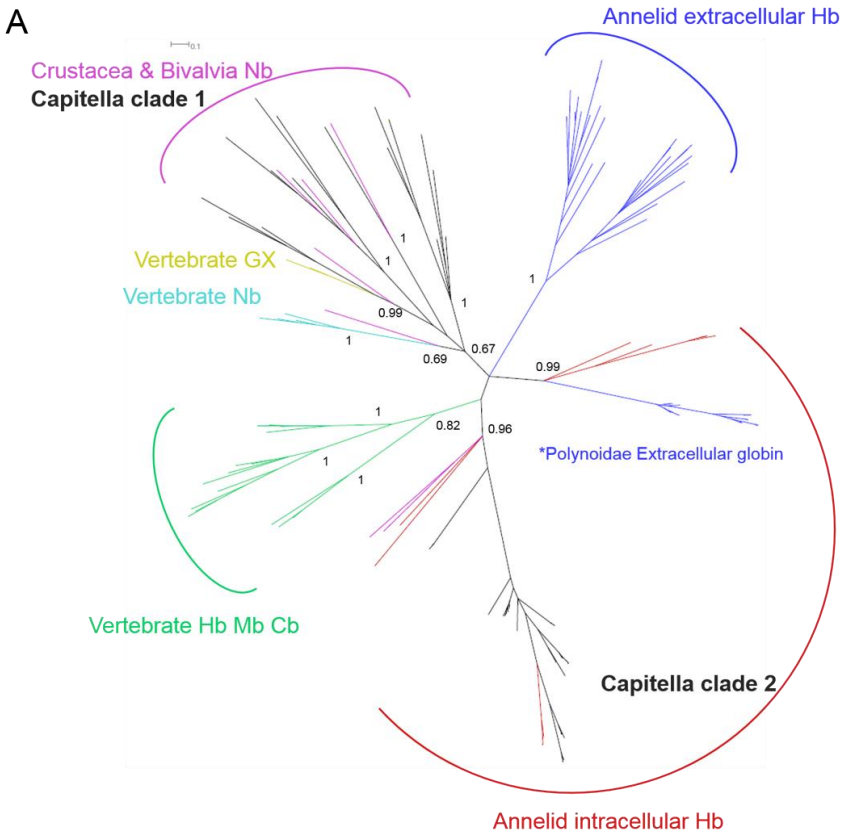
A
Annelid extracellular Hb
Crustacea & Bivalvia Nb
Capitella clade 1
Vertebrate GX
Vertebrate Nb
*Polynoidae Extracellular globin
Vertebrate Hb Mb Cb
Capitella clade 2
Annelid intracellular Hb
B
Xt_Nb
Hs_Nb
Gg_Nb
Dr_Nb
Cg_Nb1
Xt_GX
Dr_GX
CapteG188542
CapteG227018
CapteG166020
Dm_Nb2
CapteG194549
CapteG147415
Cg_Nb3
CapteG27881
Dm_Nb1
CapteG193618
CapteG214116
CapteG192439
Cg_Nb2
CapteG190593
CapteG200756
CapteG188798
CapteG195701
CapteG110047
CapteG144794
CapteG198978
CapteG98019
C
CapteG192931
CapteG132766
CapteG975
CapteG1218
CapteG817
CapteG225826
CapteG219905
CapteG21927
CapteG219237
CapteG229341
CapteG158355
CapteG184905
CapteG166267
CapteG20182
CapteG170177
CapteG114226
Uu_Hb
Uc_HbB
Uc_HbA
CapteG18433
CapteG227604
CapteG21023
CapteG225570
CapteG1470
CapteG5378
CapteG216611
CapteG21094
CapteG21508
CapteG5226
CapteG181579
CapteG218767
Ap_HbInt
Ob_Mb
Pv_Cb
Dm_Nb3

Fig. 3-3. The unrooted Bayesian phylogenic tree of globin genes
The amino acid sequence of globin genes from *Capitella teleta* and that listed in Table 3-1 were aligned by MUCLE in MEGA7. The site with lower than 80% coverage were trimmed in this alignment. The site used in this analysis was 134. The Bayesian phylogenic tree of globin genes was constructed by MrBayes 3.2.6 from 2×10^6 generation with 4 chains, estimating posterior probability from Markov chain Monte Carlo method. The LG + G model was applied to this analysis. Trees were sampled in each 100 generations and the value of burn-in was set to 2×10^5. The average standard deviation of split frequencies was 0.00979. Polynoidae extracellular globin genes are located at the same clade as annelid intracellular globin genes. This phylogeny was the same as the report in Projecto-Garcia et al. (2017) [22]. **(A)** The whole view of the Bayesian tree. **(B)** Extracted tree of Capitella clade 1. **(C)** Extracted tree of Capitella clade 2. The number showed on the node indicates the posterior probability with more than 0.7 in Fig. 3-3BC.

their expression were not affected by hypoxia. There are no evident rules in the expression of globin genes in cluster 3.

Discussion

The comparison the transcript profiles of *C. teleta* in normoxia to that in hypoxia condition provided the comprehensive understanding of the hypoxic responses in *C. teleta*. The common DEGs in the both stages were fewer than DEGs specific to each stage except for small worm-specific upregulated genes (Fig. 3-1), indicating that hypoxia-inducing responses are different in the growth stages. Moreover, the number of DEGs in large group was more than that in small group, which suggests that the larger worms would be more influenced by hypoxia. Forbes and Lopez (1990) reported that the effects of hypoxia on their growth were differ from their body size [23]. The smaller could grow up even in the hypoxic condition when they were kept in the sediment with little organic matters, while the larger could not. This difference in the influence of hypoxia is supposed to be due to the lack of blood vessels. They rely on the diffusion to acquire oxygen because of the degeneracy. Most of marine annelids inhabiting hypoxic zone bear the large gill and thick blood vessels to circulate oxygen effectively. On the other hand, *C. teleta* might have more

difficulty in the oxygen circulation as they grow up. This unique body plan possibly results in the difference of hypoxia-inducing response in growth stages.

The highly enriched GOs in response to hypoxia were largely common in both growth stages and categorize into two functions, i.e. incorporation, transportation and storage of oxygen, or enzyme, peptidase inhibitor activity (Table 3-5). GO:0004867, serine-type endopeptidase inhibitor activity was highly enriched. The most DEGs among the genes annotated as this GO were antistasin. This gene was upregulated in both growth stages by hypoxia. Antistasin was originally isolated from Hirudinia [24]. This inhibitor is known to be involved in the immune response in disk abalone [25]. The shrimp *Penaeus stylirostris* was reported to decrease in peptidase-inhibitor activity by hypoxia, increasing the resistance to viruses *via* enhancing the enzymatic immune system [26]. Hence, the enrichment of GO:004867 suggests that *C. teleta* improves immune system in response to hypoxia, especially by the upregulation of antistasin. GO:0005344, oxygen carrier activity and GO:0019825, oxygen binding were also highly enriched. The genes consisting these GO categories are globin family genes. Some globin genes were strongly downregulated in both growth stage, while some globin genes were highly upregulated in small stage.

Heat shock proteins (HSP) were highly upregulated in both growth stages by hypoxia (Tables 3-3 and 3-4). Heat shock protein family are well conserved chaperon protein, preserving the proteins from various stresses [27, 28]. Oxidative stress is one of the major stress to impair protein functions [29]. Hypoxia disturbs redox balance and results in the production of oxidative stress [30, 31]. In addition, reoxygenation also produces much oxidative stress. HSPs have a role to keep functional proteins away from oxidative stresses produced in hypoxia [32]. The upregulation of HSPs by hypoxia are observed in terrestrial animals as well as aquatic animals [10, 33-36]. *Capitella teleta* also upregulates HSPs to preserve functional proteins from oxidative stresses produced by hypoxia and reoxygenation.

The globin family is heme containing globular protein involved in oxygen transport, oxygen storage, oxidation or oxygen sensing [37]. Hypoxia influenced the expression of some globin genes annotated as hemoglobin or globin by Blast2GO (Table 3-6). To

examine the difference in the expression pattern among each group, heatmap of globin genes was constructed (Fig. 3-2). The cluster was divided into 4 categories. The globin genes in cluster 1 showed relatively high expression level in large worms during normoxia and downregulated by hypoxia. Cluster 2 genes seems to be upregulated by hypoxia in both growth stages, which suggests that globin genes functionally adaptive to hypoxia are shared throughout the growth stages. The genes in cluster 4 were relatively high expression level in small worms and their expression were not affected by hypoxia. I could not find any rules in the expression of globin genes in cluster 3.

The phylogenic analysis showed that globin genes of *C. teleta* were divided into two clades (Fig. 3-3). Both clades are located at intracellular globins. One clade constructs the clade with annelid, crustacean and molluscan intracellular globins shown as Capitella clade 1. The other clade includes vertebrate, crustacean and molluscan neuroglobin and vertebrate globin X shown as Capitella clade 2. All DEGs in globin genes were grouped into the same clade of intracellular globin genes found in annelids. The globin genes upregulated by hypoxia have high similarity with red blood cell hemoglobin of *Urechis caupo*, belonging to neighboring family of Capitellidae, Urechidae. These genes could function as red blood cell hemoglobin, which implies that *C. teleta* improves their ability for oxygen uptake and transportation to secure oxygen availability even in hypoxia. The magnitude of upregulation was higher in small worms. The smaller have advantage in oxygen availability because the length to diffuse oxygen of the smaller is less than that of the larger. However, once hypoxia occurs, the necessity to spare more effort on oxygen uptake would arise in small worms, resulting in the upregulation of more number of globin genes in small worms. On the other hand, the downregulated globin genes were found more in large group. This might be due to the difference in the necessity to express the globin genes suitable for oxygen uptake in normoxia, i.e. the larger worm usually needs more globins to keep oxygen availability throughout their body. The other clade containing neuroglobin includes no DEGs. Neuroglobin is expressed and upregulated in nerve cells by hypoxia for preventing them from the deficiency in oxygen [38, 39]. *Capitella teleta* exhibited a faint response to hypoxia in deduced neuroglobin genes. They inhabit

organically polluted sediments where DO is low throughout the year. They possibly express enough neuroglobins for oxygen storage in severe hypoxic condition even when they are in normoxia.

The influence of hypoxia on the expression pattern of globin family are observed in many aquatic animals. In *Danio rerio*, hypoxia induces downregulation of some hemoglobins, while upregulation of neuroglobin [40]. The blue crub, *Callinectes sapidus* upregulates their main respiratory pigment, hemocyanin in hypoxic condition [10, 41]. The crustacean, *Daphnia magna* highly upregulates several hemoglobin genes with difference oxygen binding ability in response to hypoxia [42, 43]. *Capitella teleta* converts the expression pattern among the globin genes, especially the gene annotated F-I hemoglobin, which is hemoglobin isolated from *U. caupo*, according to the growth stage and DO to maximize oxygen availability in any situations. This transition in molecular species of globin genes plays the key role in adaptation to hypoxia occurred in organically polluted area. Further analysis for the function and the localization of their globin genes will reveal the precise mechanism to maximize their oxygen availability in hypoxic condition.

References

1. Vaquer-Sunyer R, Duarte CM. Thresholds of hypoxia for marine biodiversity. Proc Natl Acad Sci. 2008;105: 15452–15457.
2. Vismann B. Sulfide detoxification and tolerance in *Nereis* (*Hediste*) *diversicolor* and *Nereis* (*Neanthes*) *virens* (Annelida. Polychaeta). Mar Ecol Prog Ser. 1990;59: 229–238.
3. Llanso RJ, Diaz RJ. Tolerance to low dissolved oxygen by the tubicolous polychaete *Loimia medusa.* J Mar Biol Assoc UK. 1994;74: 143.
4. Lamont PA, Gage JD. Morphological responses of macrobenthic polychaetes to low oxygen on the Oman continental slope, NW Arabian Sea. Deep Sea Res Part II Top Stud Oceanogr. 2000;47: 9–24.

5. González RR, Quiñones RA. Pyruvate oxidoreductases involved in glycolytic anaerobic metabolism of polychaetes from the continental shelf off central-south Chile. Estuar Coast Shelf Sci. 2000;51: 507–519.
6. Raps ME, Reish DJ. The effects of varying dissolved oxygen concentrations on the hemoglobin levels of the polychaetous annelid *Neanthes arenaceodentata*. Mar Biol. 1971;11: 363–368.
7. Schiedek D. *Marenzelleria viridis* (Verrill, 1873) (Polychaeta), a new benthic species within European coastal waters some metabolic features. J Exp Mar Bio Ecol. 1997;211: 85–101.
8. Schöttler U. An investigation on the anaerobic metabolism of *Nephtys hombergii* (Annelida: Polychaeta). Mar Biol. 1982;71: 265–269.
9. Quiroga E, Quiñones RA, González RR, Gallardo VA, Jessen G. Aerobic and anaerobic metabolism of *Paraprionospio pinnata* (Polychaeta: Spionidae) in central Chile. J Mar Biol Assoc UK. 2007;87: 459.
10. Sun S, Xuan F, Ge X, Fu H, Zhu J, Zhang S. Identification of differentially expressed genes in hepatopancreas of oriental river prawn, *Macrobrachium nipponense* exposed to environmental hypoxia. Gene. 2014;534: 298–306.
11. Sun S, Xuan F, Fu H, Zhu J, Ge X, Gu Z. Transciptomic and histological analysis of hepatopancreas, muscle and gill tissues of oriental river prawn (*Macrobrachium nipponense*) in response to chronic hypoxia. BMC Genomics. 2015;16: 491.
12. Sussarellu R, Fabioux C, Le Moullac G, Fleury E, Moraga D. Transcriptomic response of the Pacific oyster *Crassostrea gigas* to hypoxia. Mar Genomics. 2010;3: 133–143.
13. Zhang L, Feng Q, Ding K, Sun L, Huo D, Fang Y, et al. Genome-wide analysis of gene expression profile in the respiratory tree of sea cucumber (*Apostichopus japonicus*) in response to hypoxia conditions. J Mar Biol Assoc UK. 2018;98: 2039–2048.
14. Simakov O, Marletaz F, Cho S-J, Edsinger-Gonzales E, Havlak P, Hellsten U, et al. Insights into bilaterian evolution from three spiralian genomes. Nature. 2012;493: 526–531.

15. Patro R, Duggal G, Love MI, Irizarry RA, Kingsford C. Salmon provides fast and bias-aware quantification of transcript expression. Nat Methods. 2017;14: 417–419.
16. Soneson C, Love MI, Robinson MD. Differential analyses for RNA-seq: transcript-level estimates improve gene-level inferences. F1000Research. 2015;4: 1521.
17. Sun J, Nishiyama T, Shimizu K, Kadota K. TCC: an R package for comparing tag count data with robust normalization strategies. BMC Bioinformatics. 2013;14: 219.
18. Conesa A, Götz S, García-Gómez JM, Terol J, Talón M, Robles M. Blast2GO: a universal tool for annotation, visualization and analysis in functional genomics research. Bioinformatics. 2005;21: 3674–3676.
19. Kumar S, Stecher G, Tamura K. MEGA7: molecular evolutionary genetics analysis version 7.0 for bigger datasets. Mol Biol Evol. 2016;33: 1870–1874.
20. Ronquist F, Huelsenbeck JP. MrBayes 3: Bayesian phylogenetic inference under mixed models. Bioinformatics. 2003;19: 1572–1574.
21. Gu Z, Eils R, Schlesner M. Complex heatmaps reveal patterns and correlations in multidimensional genomic data. Bioinformatics. 2016;32: 2847–2849.
22. Projecto-Garcia J, Le Port A-S, Govindji T, Jollivet D, Schaeffer SW, Hourdez S. Evolution of single-domain globins in hydrothermal vent scale-worms. J Mol Evol. 2017;85: 172–187.
23. Forbes TL, Lopez GR. The effect of food concentration, body size, and environmental oxygen tension on the growth of the deposit-feeding polycheate, *Capitella* species 1. Limnol Oceanogr. 1990;35: 1535–1544.
24. Tuszynski GP, Gasic TB, Gasic GJ. Isolation and characterization of antistasin. An inhibitor of metastasis and coagulation. J Biol Chem. 1987;262: 9718–23.
25. Nikapitiya C, De Zoysa M, Oh C, Lee Y, Ekanayake PM, Whang I, et al. Disk abalone (*Haliotis discus discus*) expresses a novel antistasin-like serine protease inhibitor: Molecular cloning and immune response against bacterial infection. Fish Shellfish Immunol. 2010;28: 661–671.

26. Le Moullac G, Soyez C, Saulnier D, Ansquer D, Avarre JC, Levy P. Effect of hypoxic stress on the immune response and the resistance to vibriosis of the shrimp *Penaeus stylirostris*. Fish Shellfish Immunol. 1998;8: 621–629.
27. Feder ME, Hofmann GE. Heat-shock proteins, molecular chaperons, and the stress response: evolutionary and ecological physiology. Annu Rev Physiol. 1999;61: 243–282.
28. Parsell D. The function of heat-shock proteins in stress tolerance: degradation and reactivation of damaged proteins. Annu Rev Genet. 1993;27: 437–496.
29. Finkel T, Holbrook NJ. Oxidants, oxidative stress and the biology of ageing. Nature. 2000;408: 239–47.
30. Prabakaran S, Swatton JE, Ryan MM, Huffaker SJ, Huang J-J, Griffin JL, et al. Mitochondrial dysfunction in schizophrenia: evidence for compromised brain metabolism and oxidative stress. Mol Psychiatry. 2004;9: 684–697.
31. Pialoux V, Hanly PJ, Foster GE, Brugniaux J V., Beaudin AE, Hartmann SE, et al. Effects of exposure to intermittent hypoxia on oxidative stress and acute hypoxic ventilatory response in humans. Am J Respir Crit Care Med. 2009;180: 1002–1009.
32. Taylor L, Midgley AW, Chrismas B, Madden LA, Vince R V., McNaughton LR. The effect of acute hypoxia on heat shock protein 72 expression and oxidative stress in vivo. Eur J Appl Physiol. 2010;109: 849–855.
33. Mestril R, Chi SH, Sayen MR, Dillmann WH. Isolation of a novel inducible rat heat-shock protein (HSP70) gene and its expression during ischaemia/hypoxia and heat shock. Biochem J. 1994;298: 561–569.
34. Shen C, Nettleton D, Jiang M, Kim SK, Powell-Coffman JA. Roles of the HIF-1 hypoxia-inducible factor during hypoxia response in *Caenorhabditis elegans*. J Biol Chem. 2005;280: 20580–20588.
35. Baird NA, Turnbull DW, Johnson EA. Induction of the heat shock pathway during hypoxia requires regulation of heat shock factor by hypoxia-inducible factor-1. J Biol Chem. 2006;281: 38675–38681.

36. Delaney MA, Klesius PH. Hypoxic conditions induce Hsp70 production in blood, brain and head kidney of juvenile Nile tilapia *Oreochromis niloticus* (L.). Aquaculture. 2004;236: 633–644.
37. Vinogradov SN, Moens L. Diversity of globin function: enzymatic, transport, storage, and sensing. J Biol Chem. 2008;283: 8773–8777.
38. Dewilde S, Kiger L, Burmester T, Hankeln T, Baudin-Creuza V, Aerts T, et al. Biochemical characterization and ligand binding properties of neuroglobin, a novel member of the globin family. J Biol Chem. 2001;276: 38949–38955.
39. Sun Y, Jin K, Mao XO, Zhu Y, Greenberg DA. Neuroglobin is up-regulated by and protects neurons from hypoxic-ischemic injury. Proc Natl Acad Sci. 2001;98: 15306–15311.
40. Roesner A. Hypoxia induces a complex response of globin expression in zebrafish (*Danio rerio*). J Exp Biol. 2006;209: 2129–2137.
41. Brouwer M, Larkin P, Brown-Peterson N, King C, Manning S, Denslow N. Effects of hypoxia on gene and protein expression in the blue crab, *Callinectes sapidus*. Mar Environ Res. 2004;58: 787–792.
42. Kimura S, Tokishita S, Ohta T, Kobayashi M, Yamagata H. Heterogeneity and differential expression under hypoxia of two-domain hemoglobin chains in the water flea, *Daphnia magna*. J Biol Chem. 1999;274: 10649–10653.
43. Zeis B, Becher B, Lamkemeyer T, Rolf S, Pirow R, Paul RJ. The process of hypoxic induction of *Daphnia magna* hemoglobin: subunit composition and functional properties. Comp Biochem Physiol Part B Biochem Mol Biol. 2003;134: 243–252.

General discussion

I demonstrated that *P. hessleri* escapes acids and oxidative stress with higher sensitivity than shallow species does, and that *C. teleta* evacuates from the burrow in response to hypoxia. Pharmacological tests showed that these avoidance behaviors from environmental stresses are mediated by TRP channels. In addition to this, I illustrated the comprehensive transcriptomic responses to hypoxia in *C. teleta*, i.e. they improve the ability to prevent functional proteins from oxidative stresses produced by hypoxia and reoxygenation, and to acquire oxygen by changing molecular species of globins. Environmental adaptations of organisms have often been considered from the three point of view, morphological, physiological and behavioral adaptation. However, this study indicates that sensory adaptation also plays an important role in environmental adaption because the function for sensing environmental factors is to perceive precisely the range of survival limits and to regulate physiology and behavior in response to the environmental changes.

Sensory adaptations are occurred in both intraspecies and interspecies manners. Intraspecies sensory adaptations are described as plasticity in some studies. The mantis shrimp, *Haptosquilla trispinosa*, tunes the color perception in accordance with the local light environments [1]. *Caenorhabditis elegans* adapts volatile attractants for several hours. They show the diminishment of the chemotaxis in odorant-dependent manner partially mediated by OSM-9, a member of TRP channels [2]. Interspecies sensory adaptation has been described in temperature sensation. The study comparing the temperature sensation in two frogs, *Xenopus tropicalis* and *X. laevis* shows the habitat-reflecting shift in thermal sensation mediated by thermo-sensitive TRP channels [3]. In this study, I examined the adaptation mechanism of marine annelids to harsh environments, deep-sea hydrothermal vent and hypoxic zone. I demonstrated that TRP channels of the marine annelids examined have an important role for sensing the key environmental factor, acids and oxidative stress in hydrothermal vents and hypoxia in organically polluted area. Moreover, the interspecies sensory adaptation of TRP channels in *P. hessleri* are shown, although the tuning of TRPA

homologue in *C. teleta* to hypoxic environments have not been examined. This study shed a new light on the function of TRP channels as a key driver of sensory adaptation among marine animals.

In decades, marine environments have been globally changed by anthropogenic activity. Ocean acidification, eutrophication, warming and hypoxia are observed and may cause various effects on marine ecosystems [4-7]. The achievement of this study demonstrating molecular responses of the major maintainer in seafloor, marine annelids, to environmental factors may help to forecast the impacts of the changes in marine environments on marine ecosystems.

References

1. Cronin TW, Caldwell RL, Marshall J. Tunable colour vision in a mantis shrimp. Nature. 2001;411: 547–548.
2. Colbert HA, Bargmann CI. Odorant-specific adaptation pathways generate olfactory plasticity in *C. elegans*. Neuron. 1995;14: 803–12.
3. Saito S, Ohkita M, Saito CT, Takahashi K, Tominaga M, Ohta T. Evolution of heat sensors drove shifts in thermosensation between *Xenopus* species adapted to different thermal niches. J Biol Chem. 2016;291: 11446–11459.
4. Fabry VJ, Seibel BA, Feely RA, Orr JC. Impacts of ocean acidification on marine fauna and ecosystem processes. ICES J Mar Sci. 2008;65: 414–432.
5. Cloern J. Our evolving conceptual model of the coastal eutrophication problem. Mar Ecol Prog Ser. 2001;210: 223–253.
6. Levitus S, Antonov JI, Boyer TP, Stephens C. Warming of the world ocean. Science. 2000;287: 2225–2229.
7. Breitburg D, Levin LA, Oschlies A, Grégoire M, Chavez FP, Conley DJ, et al. Declining oxygen in the global ocean and coastal waters. Science. 2018;359: eaam7240.

Acknowledgements

I am grateful to Dr. Haruhiko Toyohara for the scientific supports throughout my research life in this laboratory and for teaching me what researcher is.

I would like to thank Dr. Kenji Sato and Dr. Masato Kinoshita for much advice on my research as well as my private life.

My appreciation goes to Dr. Shingo Maegawa from Kyoto University for helping me with constructing the basis of molecular biology and experimental techniques and for critical advice on my research. I would like to thank Dr. Hiroshi Hosokawa from Kyoto University for giving me the opportunity to conceiving of the research idea in Ph.D. thesis.

I also thank to Dr. Hiroaki Tsutsumi from Kumamoto Prefectural University and Dr. Naoko Ueda from the University of Kitakyushu for giving me the stock culture of *Capitella teleta* and much advices on the rearing of *C. teleta*.

I would like to express my gratitude to Dr. Shuichi Shigeno from the University of Chicago, previously from Japan Agency for Marine-Earth Science and Technology, for constructing research plan to study the adaptation mechanism of *Paralvinella hessleri* to deep-sea hydrothermal vents and giving much information about it. I also thank to Dr. Katsunori Fujikura from Japan Agency for Marine-Earth Science and Technology for supporting this research and reviewing my first paper.

I would like to thank Dr. Koji Inoue from Tokyo University and Dr. Tomoko Koito from Nihon University for giving me the opportunity to conduct experiments on board research vessels, Kaiyo. I also thank the crews and staffs of RV Natsushima and RV Kaiyo, and ROV Hyper-Dolphin during cruise NT12-10 and KY15-07.

I am deeply grateful to Dr. Makoto Tominaga, Dr. Yoshiro Suzuki, Dr. Shigeru Saito, Dr. Takaaki Sokabe and all staff from Thermal Biology Group, Exploratory Research Center on Life and Living Systems for giving me an opportunity to analyze the function of marine annelids' TRP channels.

Finally, I would like to thank the past and present members of laboratory of Marine Biological Function for supporting my research life.

This study is partially supported by Grant-in-Aid for JSPS Research Fellow (Grant number 16J11123).